The predominant cAMP-stimulated 3·5 kb StAR mRNA contains specific sequence elements in the extended 3′UTR that confer high basal instability

Haichuan Duan[1] and **Colin R Jefcoate**

Department of Pharmacology, University of Wisconsin-Madison Medical School, 1300 University Avenue, Madison, Wisconsin-Madison 53706, USA

[1]Molecular and Cellular Pharmacology Graduate Program, University of Wisconsin-Madison, Madison, USA

(Requests for offprints should be addressed to C R Jefcoate; Email: jefcoate@wisc.edu)

Abstract

cAMP stimulation of rodent steroidogenic cells produces two StAR transcripts, a major 3·5 kb and a minor 1·6 kb mRNA, differing only in their 3′ untranslated regions (3′UTR). They exhibit very different responses to stimulation and removal of 8-Br-cAMP, with the 3·5 kb form increasing and declining much more rapidly than the 1·6 kb form. The 3′ end of the 3·5 kb StAR mRNA contains three conserved AU-rich element (AURE) motifs that mediate fast mRNA turnover in over 900 genes in the human genome. In this paper, we explore post-transcriptional regulation in steroidogenic and non-steroidogenic cells using expression vectors containing StAR or luciferase with different StAR 3′UTRs. We show that the basal steady-state levels of StAR or luciferase protein and mRNA are five to eight times lower with the 3′UTR of 3·5 kb StAR compared with that of the 1·6 kb 3′UTR. Examination of transcript stability by direct mRNA transfection showed only a 1·5-fold increase in the rate of cytoplasmic decay of the 3·5 kb mRNA relative to the 1·6 kb mRNA. However, the long 3′UTR caused a fivefold decrease in the rate of appearance of mature cytoplasmic mRNA despite transcription from the same promoter. This is attributed to less efficient nuclear processing of immature transcripts prior to export to cytoplasm. Selective 3′UTR sequence substitutions, deletions, and mutations showed that this loss of expression is produced additively by specific sequences in a 700-base basal instability region and by non-specific length effects. These mechanisms are selectively enhanced in steroidogenic cells. The AURE contribute a smaller basal destabilization effect selective for steroidogenic cells that is removed by their mutations. Inclusion of introns in the 3·5 kb StAR vector enhances StAR expression, suggesting the effects of introns complexes on nuclear processing. Br-cAMP provides an additional means to rapidly modulate StAR expression independent of transcription by attenuating the nuclear and cytoplasmic instability mechanisms within the extended 3′UTR.

Journal of Molecular Endocrinology (2007) **38,** 159–179

Introduction

The steroidogenic acute regulatory protein (StAR) is a critical mediator of intramitochondrial cholesterol transport, a rate-limiting step in tropic hormone-activated steroidogenesis (Krueger & Orme-Johnson 1983, Pon *et al.* 1986, Epstein & Orme-Johnson 1991, Clark *et al.* 1994, Sugawara *et al.* 1995). StAR is hormonally regulated in essentially all cell types that convert cholesterol to steroid hormones. In adrenal cells, adrenocorticotropic hormone (ACTH) increases glucocorticoids within a few minutes as part of the acute response to stress. cAMP stimulates rapid and substantial increases of StAR mRNA in rat adrenals *in vivo* and in steroidogenic mouse Y-1 and MA-10 cells *in vitro* (Clark *et al.* 1995, Ariyoshi *et al.* 1998).

The acute stimulation phase involves regulation of both mRNA levels and several additional processes. Synthesized as a 37 kDa precursor (p37), StAR is imported into mitochondria where its leader sequence is cleaved by mitochondrial proteases to generate a series of 28–30 kDa forms. The C-terminus of StAR harbors a cholesterol-binding START domain (Tsujishita & Hurley 2000). Studies using non-steroidogenic COS-1 cells indicate that StAR can function at the outer mitochondrial membrane (Arakane *et al.* 1996). However, in much more active steroidogenic cells, StAR needs to be continually translated and imported into mitochondria to be optimally effective (Ferguson 1963, Privalle *et al.* 1983, Epstein & Orme-Johnson 1991, Stocco & Sodeman 1991, King *et al.* 1999, Artemenko *et al.* 2001, Bose *et al.* 2002). Functionally disruptive mutations of *StAR* gene cause the congenital lipoid adrenal hyperplasia disease in human (Fujieda *et al.* 2003), and similar phenotypes are observed in StAR null mice (Caron *et al.* 1997). Several other proteins have also been implicated in cholesterol delivery to the inner membrane cytochrome P450scc. These include the peripheral-type benzodiazepine receptor (PBR), an interacting protein PAP7, an additional StAR-binding protein and enzymes

0952–5041/07/038–159
DOI: 10.1677/jme.1.02153
Online version via http://www.endocrinology-journals.org

involved in fatty acid delivery to mitochondria (Liu *et al.* 2003, Sugawara *et al.* 2003, Cornejo Maciel *et al.* 2005, Hauet *et al.* 2005). Processes involved in the delivery of cholesterol to mitochondria are also critical to the activation of steroidogenesis. These include activation of hormone-sensitive lipase and suppression of acyl CoA: cholesterol acyltransferase (ACAT) by tropic hormones (DiBartolomeis & Jefcoate 1984, Temel *et al.* 1997, Buhman *et al.* 2000, Kraemer *et al.* 2004).

In mouse and rat steroidogenic cells, two predominant forms of StAR transcripts of 1·6 and 3·5 kb are expressed (Clark *et al.* 1995). A minor 2·8 kb form reported earlier was not consistently detected in our experiments. We have shown that the two major transcripts arise from alternative use of polyadenylation signals in exon 7 (Ariyoshi *et al.* 1998). The two transcripts share the same 5′UTR and open reading frame, only differing in their 3′UTR. The 3·5 kb transcript has an extended 3′UTR not present in the 1·6 kb transcript (Fig. 1). Several AUUUA motifs are found at the 3′ end of the 3·5 kb transcript. In an earlier publication, we found that the two messages are regulated differently by mRNA stability mechanisms through their 3′UTRs (Zhao *et al.* 2005). The abundance of an mRNA species is determined by multiple processes, including transcription, pre-mRNA processing, nuclear export, and cytoplasmic turnover. In particular, transcript stability is an important control point of its expression level. The half-lives of mammalian mRNAs range from <20 min to over 24 h, and can readily be altered by external stimuli. An increase in the stability of a labile mRNA can provide a faster response than transcriptional regulation.

Previous work has extensively addressed the transcriptional regulation of StAR. Numerous transcription factors have been identified to interact with sites within the StAR promoter. These include both positive regulators, such as SF-1, C/EBP, GATA, SREBP, Sp1, CREB/CREM, and AP-1 and negative regulators, such as DAX-1 and YY1 (Manna *et al.* 2003). Another important regulatory mechanism of StAR transcription involves acetylation and methylation of histones bound to StAR promoter (Sun *et al.* 2003, Hiroi *et al.* 2004, Rusovici *et al.* 2005). Recently, a corepressor complex of mSin3A–HDAC1/2 has been identified to associate with Sp3 and CAGA element-binding proteins on the StAR promoter (Clem & Clark 2006).

Regulation of mRNA stability provides yet another mechanism that also addresses the independent regulation of the different StAR transcripts. Sequence elements that stabilize or destabilize a transcript can occur in its 5′UTR, open reading frame, or 3′UTR (Guhaniyogi & Brewer 2001). Among the best studied and most prevalent of these is the AU-rich element (AURE), present in the 3′UTR of many labile cytokine and proto-oncogene mRNAs. Several classes of AURE have been described, which contain clustered or distributed AUUUA pentameric motifs or a U-rich sequence (Brennan & Steitz 2001). AURE mediate rapid turnover of transcripts as well as their stabilization or destabilization by signal transduction pathways. Multiple AURE-interacting proteins with opposing effects on mRNA stability have been identified, such as AUF-1, TTP, KSRP (destabilizing), and HuR (stabilizing). These factors function by either recruiting mRNA metabolizing machineries or protecting the message from enzymatic degradation (Bevilacqua *et al.* 2003). Signal transduction pathways change decay rates of AURE-containing transcripts through altering binding properties of AURE-interacting proteins (Wilusz & Wilusz 2004).

In addition to the cytoplasmic stability regulation, the decay of nuclear RNA is an important and highly regulated process for ensuring mature mRNA quality (Moore 2002). Inefficiently processed, unpolyadenylated or erroneously transcribed messages are targeted for degradation by the nuclear exosome (Vinciguerra & Stutz 2004). Introns also impact the nuclear retention and subsequent decay of nascent transcripts (Le Hir *et al.* 2003). The packaging of ribonucleoprotein complexes is initiated on intron sequences, thus enhancing the possibility of degradation of simple cDNA transcripts.

The majority of genes that are controlled at the mRNA stability level are needed for acute cellular responses to stimuli, such as early response genes, cytokines, and inflammatory mediators. The predominance of the less stable 3·5 kb StAR provides the opportunity for similar acute regulations. A key feature of regulation through mRNA stability is that the mRNA is unstable under basal conditions such that stabilization enhances its expression. In this paper, we show

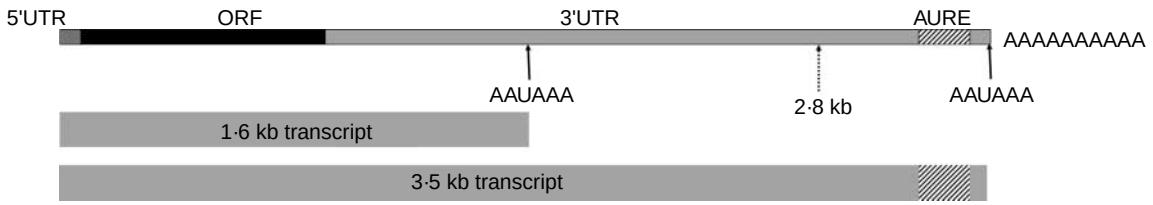

Figure 1 Diagram showing the two StAR transcripts expressed in rodent steroidogenic cells. They arise from different use of AAUAAA polyadenylation signals and differ only in their 3′UTRs. An AU-rich element is found only at the 3′ end of the 3·5 kb transcript. ORF, open reading frame.

that the 3·5 kb mRNA provides this basal instability and resolve contributions of the 3′UTR sequence elements that are responsible for differential regulation of basal stability of StAR transcripts. To this end, StAR and luciferase expression vectors with short or long 3′UTR sequences were constructed. We used these vectors to separate non-specific and sequence-specific effects on StAR mRNA and protein expression levels within the 3′UTR. We also introduced mutations into AURE motifs to elucidate their contributions. Comparisons of StAR and luciferase chimeras were used to check the effects of StAR 5′UTR and open reading frame (ORF). These effects were examined in non-steroidogenic COS-1 cells and in steroidogenic Y-1 and MA-10 cells. We employed different approaches to study StAR mRNA stability, based on steady-state expression from cytomegalovirus (CMV) promoter constructs and direct measurement of transfected mRNA half-life. The steady-state differences in protein and mRNA expression caused by the extended 3′UTR were far greater than the differences in mRNA stability. To further examine whether this effect of 3′UTR was related to post-transcriptional nuclear events, we used isopropyl-beta-D-thiogalactopyranoside (IPTG)-inducible luciferase chimeras to measure the effect of 3′UTR on kinetics of luciferase appearance in the cytoplasm. The well-established role of introns in nuclear events also led us to compare the expression of StAR from a full length construct with or without the six introns.

Materials and methods

Materials

Chemicals were obtained from Sigma Chemical Company at the highest grade unless otherwise stated. Cell culture media and horse serum were bought from Invitrogen/GIBCO Company. Fetal bovine serum was purchased through Atlanta Biologicals, Inc. (Lawrenceville, GA, USA). The *Trans*It-LT1 reagent for DNA vector transfection and *Trans*It-mRNA kit for mRNA transfection were from Mirus Bio Corporation (Madison, WI, USA). Pfu Ultra enzyme for PCR cloning was purchased from Stratagene (La Jolla, CA, USA). Restriction enzymes were purchased from Promega. Plasmid and RNA preparation kits were purchased from Qiagen. Cell culture flasks, dishes, and plates were purchased from Corning, Inc. (Corning, NY, USA).

Plasmid constructs

Primers for cloning were all designed with a 5′ overhang of four to six bases, followed by the appropriate restriction sites, and a 25–30 base region that complements the original vector at the 3′ end.

Rat and mouse StAR expression constructs are derived from the pCINeo mammalian expression vector (Promega) driven by a CMV promoter. The 1·6 and 3·5 kb rat StAR constructs were described previously (Zhao *et al.* 2005). To make the StAR construct without the 3′UTR (StARdUTR, Fig. 2A), the primer pair 5′-AGCTCTCGAGGA ACAAATCCCT GGGAGCA G-3′ and 5′-GGTGTCTAGACCTTAACACTGGGCCTCA GA-3′ were used to amplify StAR3.5k vector. The PCR product was cut with XhoI/XbaI and ligated into pCINeo. Mouse StAR vectors mStARdUTR, mStAR1.6k, and mStAR3.5k were made by amplifying mouse cDNA (isolated from Y-1 cells) with the forward primer 5′-TA GTCTAGATCAGGACCTTGAAAGGCTCAGG-3′ and reverse primers 5′-GTGGCGGCCGCTTAACACTGGG CCTCAGAGGCA-3′, 5′-CTGGCGGCCGCATGTATGTT CTTTATTGTCATG-3′ and 5′-TAGGCGGCCGCATGCC AGTGACAACTGCTTTTA-3′ respectively. PCR products were digested by XbaI/NotI and ligated into the XbaI/NotI sites of pCINeo. To make mStAR3.5/introns vector, the primers 5′-CAGCACGCGTACTCAGGACC TTGAAAGGCTCAGGA-3′ and 5′-CCCATCTAGAGAAT-GACTATTAACACAATTTAATA-3′ were used to do long-range amplification of mouse genomic DNA (isolated from Y-1 cells). The resulting 7·5 kb mouse *StAR* gene was digested with MluI/XbaI and ligated into the MluI/XbaI sites of pCINeo.

Luciferase chimeric constructs were made by inserting rat StAR 3′UTR sequences after *luc*+ORF. To make UTRS and UTRSas (Fig. 3A), the primers 5′-CCAGAC-TAGTGGACTGCCCACCACATCTAC-3′ and 5′-TTAG-ACTAGTGTCTATTAACGTCAAATGAC-3′ were used to amplify StAR3.5k vector; for UTRL and UTRLas, 5′-CC AGACTAGTGGACTGCCCACCACATCTAC-3′ and 5′–TGTCACTAGTACCTATAATCAGACTGCCAAT-3′ were used; for UTRdARE, 5′-CCAGACTAGTGGACTGCCC ACCACATCTAC-3′ and 5′-TCATACTAGTGCGC AGTCCTTGCAGGTGAT-3′ were used; for vector 684-2115 and 684-2115as (Fig. 4A), 5′-AGAACTAGT CCTAAAAATGTAATTTCATAACAAACAC-3′ and 5′-GA CACTAGTCTCGGAGGGACAGAAAAGTGGGCCA-3′ were used. PCR products were digested with SpeI and ligated to the XbaI site after *luc*+. Insert directions were determined by sequencing.

The vector ARE (Fig. 5A) was generated using the primers 5′-CCACTGCAGTTACACGGCGATCTTTCC GCCCTTC-3′ and 5′-CCCCTGCAGTAAACGGTCTTA GTCGTCTGGGTCC-3′ to amplify UTRL, after which the PCR product was digested with PstI and self-ligated. Constructs 684-1043, 684-1403, and 684-1763 (Fig. 6A) were made by amplifying 684-2115 using the forward primer 5′-AGACTGCAGTCGGGGCGGCCGGCCG-CTTCGAGC-3′ and reverse primers 5′-GGACTGC-AGTGTCCACTAAGGCTACAATAGGGCA-3′, 5′-GAC-CTGCAGTCTGTTACCAACTGACCTCATAAAC-3′, 5′-TCTCTGCAGCTTCCTGGAGTCTTCCCTCTTTGTG-3′

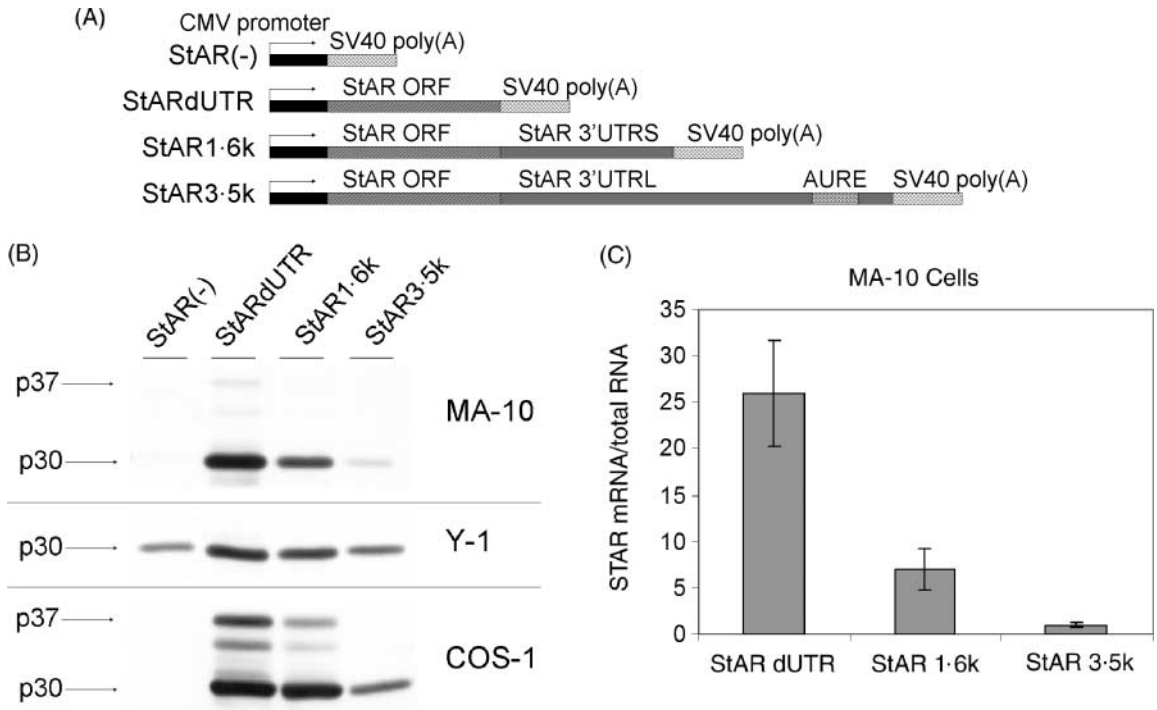

Figure 2 Effects of StAR 3′UTR on basal expression in StAR cDNA constructs. (A) Diagram showing empty vector (pCINeo) or StAR expression vectors with different 3′UTRs. (B) Western blot of StAR protein in MA-10, Y-1, and COS-1 cells transfected with these vectors. The experiment was repeated thrice with similar results. (C) StAR mRNA levels in MA-10 cells transfected with these vectors are determined by real-time RT-PCR. Data are means ± S.D. from two experiments.

respectively. PCR products using these primer pairs were digested with PstI and self-ligated. The vector 1043-1763 was made by amplifying 684-1763 using primers 5′-TAGTCTAGACCAGGCTCCCACATGGTACACAGAC-3′ and 5′-AGGTCTAGAATTACACGGCGATCTTTCCGCCCTT-3′. PCR product was digested with XbaI and self-ligated. The vector 1043-1763as was made by amplifying 684-1763 using primers 5′-TAATCTGCAGCCAGGCTCCCACATGGTACACAG-3′ and 5′-CCGATCTAGACTTCCTGGAGTCTTCCCTCTTTG-3′. PCR product was digested with PstI/XbaI and ligated into PstI/XbaI digested 684-1763 vector backbone.

Constructs for *in vitro* transcription of rat StAR messages were made from pBSKpA.1B with a T7 promoter and 90-base synthetic poly(A) tail (Dr James Malter, University of Wisconsin-Madison). StARdUTR, StAR1.6k, and StAR3.5k inserts were cloned by amplifying StAR3.5k vector with the forward primer 5′-TATCCCGGGAAGAACAAATCCCTGGGAGC-3′ and reverse primers 5′-ATACCCGGGTTAACACTGGGCCTCAGAGG-3′, 5′-TTACCCGGGAGTCTATTAACGTCAAATGAC-3′ and 5′-TTTCCCGGGACCTATAATCAGACTGCCAAT-3′ respectively. PCR products were digested by SmaI and ligated into the SmaI site of pBSKpA.1B.

IPTG-inducible luciferase vectors were made by introducing inserts into pOPRSVI/MCS (Stratagene). For LacLuc (Fig. 7B), the primers 5′-TGGCTCGAGGGTACTGTTGGTAAAGCCACC-3′ and 5′-GACTCTAGAATTACACGGCGATCTT-3′ were used to amplify the pGL3-promoter vector. PCR product was digested with XhoI/XbaI and ligated to the XhoI/XbaI sites within pOPRSVI/MCS. For LacLuc–UTRS, 5′-TGGCTCGAGGGTACTGTTGGTAAAGCCACC-3′ and 5′-CCCGCGGCCGCTGTCTATTAACGTCAAATGAC-3′ were used to amplify UTRS; for LacLuc–UTRL, 5′-TGGCTCGAGGGTACTGTTGGTAAAGCCACC-3′ and 5′-CCCGCGGCCGCTACCTATAATCAGACTGCCAAT-3′ were used to amplify UTRL. PCR products were digested by XhoI/NotI and ligated to the XhoI/NotI sites within pOPRSVI/MCS.

All constructs were sequenced using appropriate primers to ensure that the inserts are correct.

Cell culture and DNA vector transfection

Y-1 mouse adrenocortical tumor cells were expanded from a subclone obtained from Dr Bernard Schimmer (University of Toronto) that has a lower passage number than those available from ATCC. They were cultured in F-12K media (Sigma) supplemented with 15% horse serum, 2·5% fetal bovine serum, 17·86 mM $NaHCO_3$, 50 IU penicillin, and 50 μg/ml streptomycin. MA-10 mouse Leydig tumor cells were a generous gift

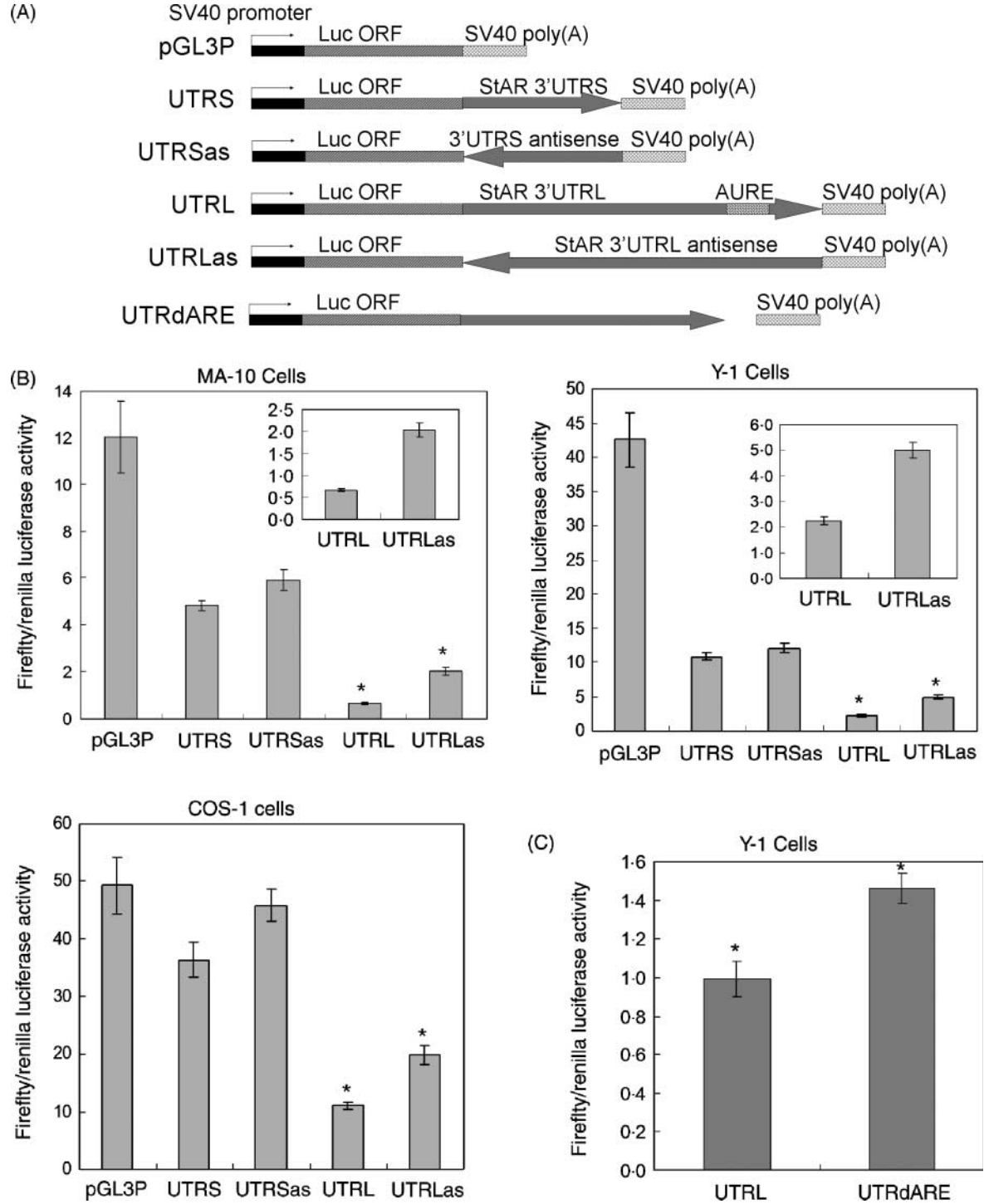

Figure 3 Comparison of luciferase constructs with sense, antisense 3′UTRs, and AURE deletion. (A) Diagram showing luciferase vectors with sense and antisense insertions, as well as AURE deletion. (B) and (C) Vectors shown in (A) were cotransfected with the control vector pRLTK into MA-10, Y-1, or COS-1 cells. Firefly and renilla luciferase activities were measured. Data represent mean ± S.D. from three transfections. The experiment was repeated two to three times with similar results. $^{*}P<0{\cdot}01$ for the pair by Student's *t*-test.

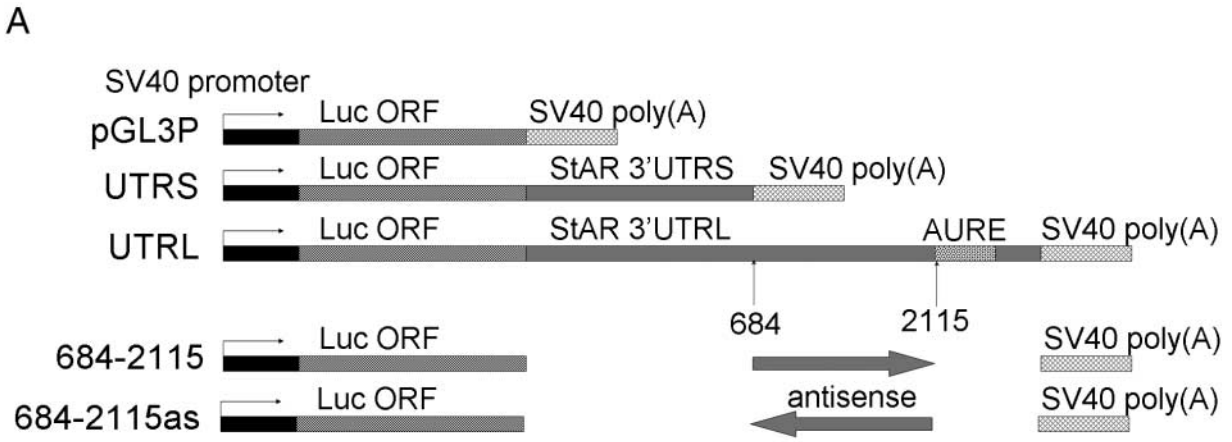

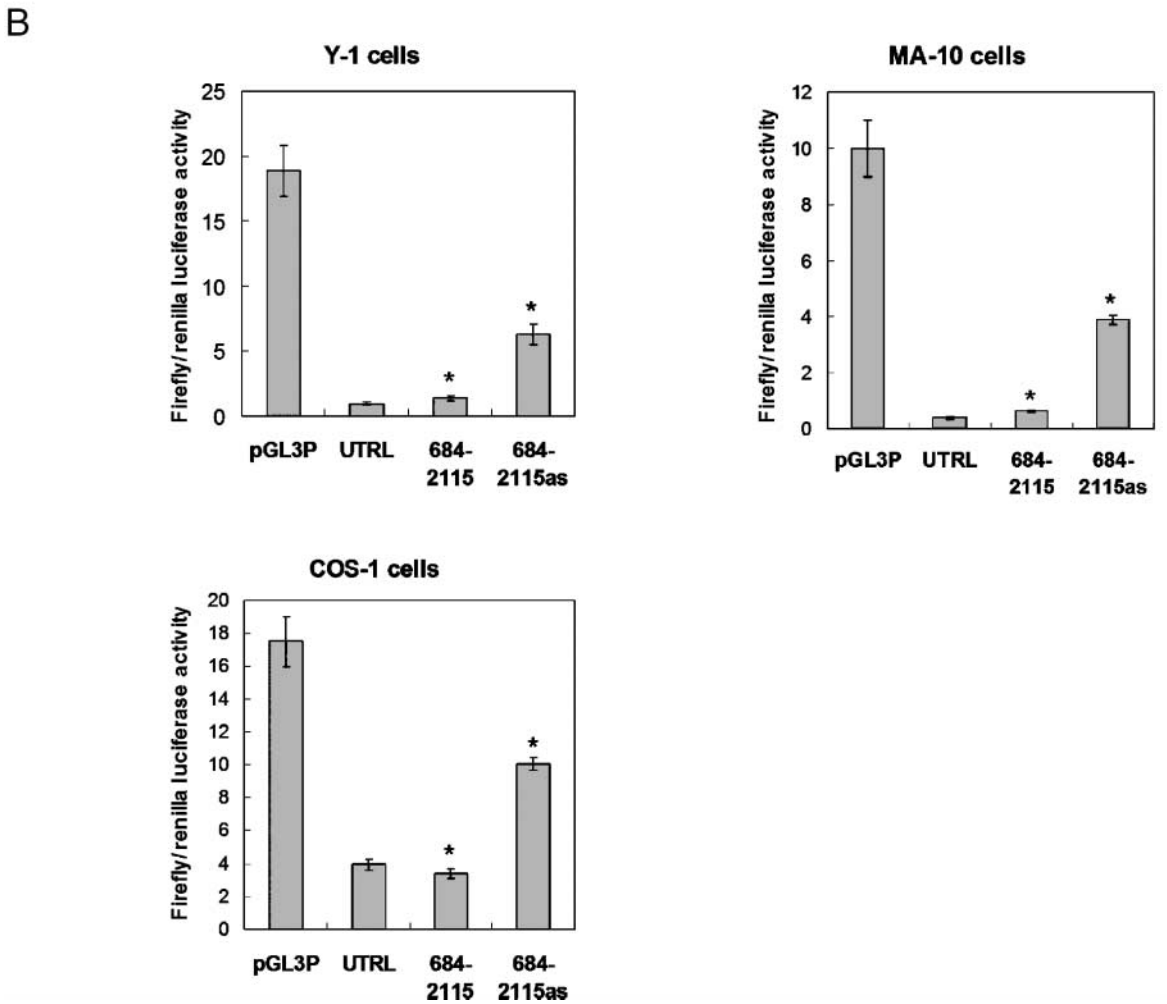

Figure 4 Upstream region effects on luciferase basal expression. (A) Diagram showing luciferase vectors to examine destabilizing effects of the upstream region. (B) Vectors in (A) were cotransfected with the control vector pRLTK into steroidogenic Y-1, MA-10, and non-steroidogenic COS-1 cells. Firefly and renilla luciferase activities were measured. Data represent means ± S.D. from three transfections. The experiment was repeated thrice with similar results. *$P < 0{\cdot}01$ by Student's *t*-test for the pair.

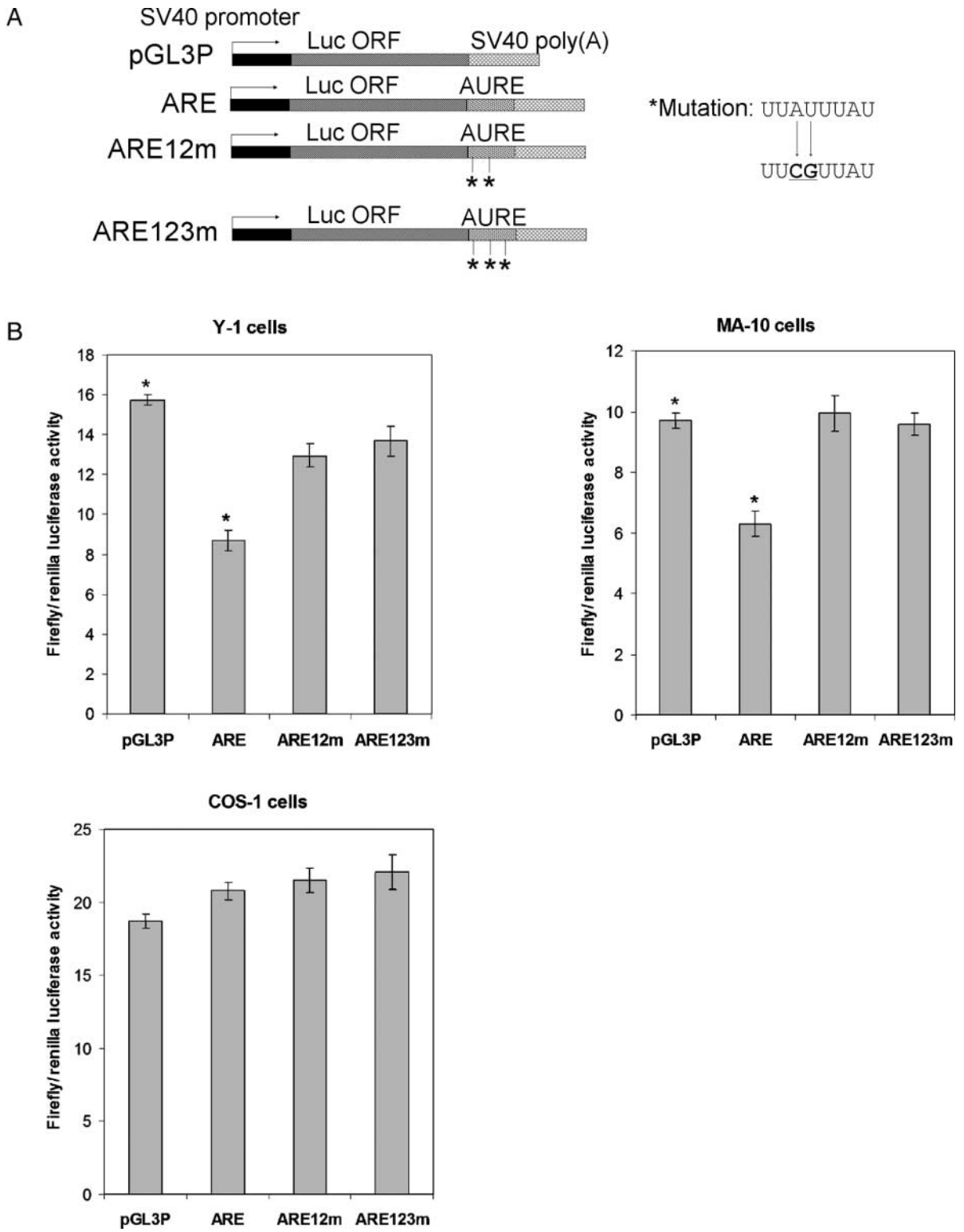

Figure 5 Effects of AURE mutations on luciferase basal expression. (A) Diagram showing the wild-type AURE as well as mutant AURE vectors. (B) Vectors in (A) were cotransfected with the control vector pRLTK into steroidogenic Y-1, MA-10, and non-steroi dogenic COS-1 cells. Firefly and renilla luciferase activities were measured. Data represent means ± S.D. from three transfections. The experiment was repeated thrice with similar results. *$P<0{\cdot}001$ by Student's *t*-test for the pair.

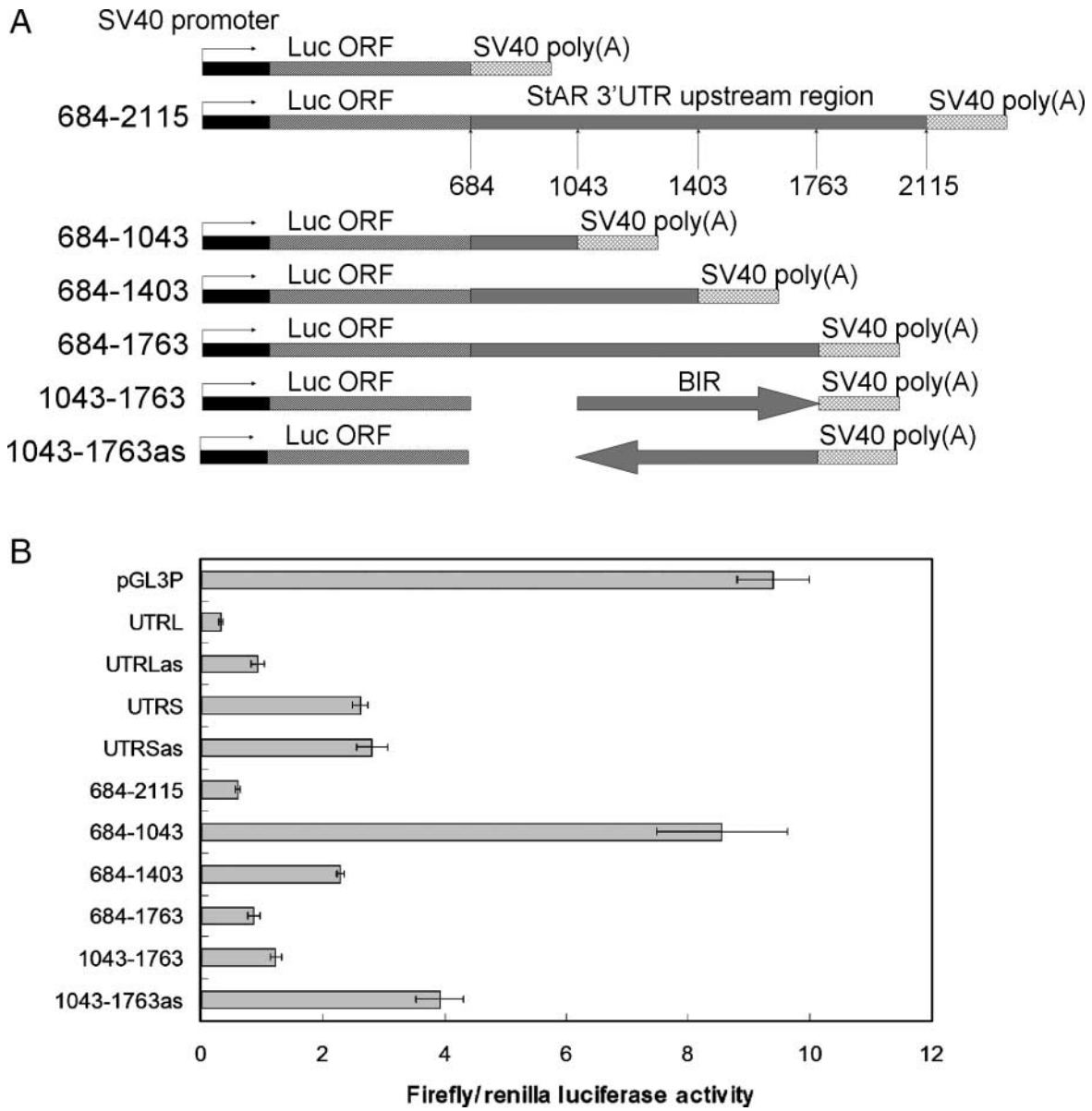

Figure 6 Identification of the basal instability region (BIR). (A) Diagram showing serial deletion vectors to examine upstream region sequences. (B) Vectors in (A) as well as previously shown were cotransfected with the control vector pRLTK into MA-10 cells. Firefly and renilla luciferase activities were measured. Data represent means ± S.D. from three transfections. The experiment was repeated thrice with similar results.

from Dr Mario Ascoli (University of Iowa College of Medicine). They were maintained in D-MEM/F-12 media (GIBCO) supplemented with 5% horse serum, 2·5% fetal bovine serum, 26·66 mM $NaHCO_3$, and 50 μg/ml gentamicin. To ensure consistent good growth, MA-10 cells were cultured on 0·1% gelatin-coated plates (Hirakawa *et al.* 2002). COS-1 cells were purchased from ATCC and cultured in D-MEM with high glucose, L-glutamine, and sodium pyruvate (GIBCO), supplemented with 10% fetal bovine serum, 17·86 mM $NaHCO_3$, 50 IU penicillin, and 50 μg/ml streptomycin. All cells were incubated at 37 °C in a humidified atmosphere with 5% CO_2.

StAR and luciferase expression vectors were transfected with *Trans*It-LT1 (Mirus Bio Corp.) according to manufacturer's protocol. Briefly, cells were seeded in 24- or 6-well plates at 25% density 24 h prior to transfection. Triplicate cultures were transfected with

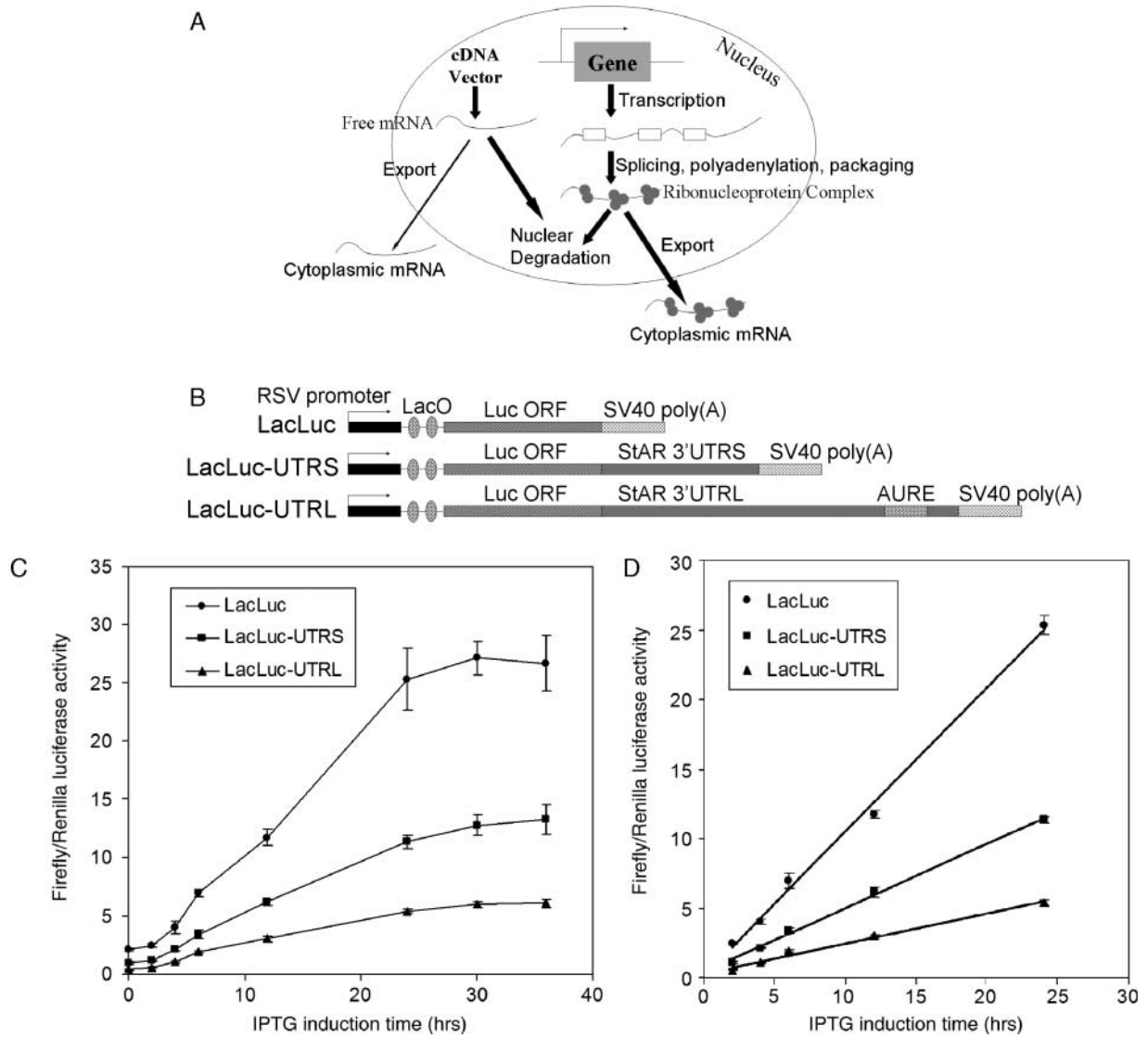

Figure 7 Effects of StAR 3′UTR on mature cytoplasmic mRNA synthesis rates. (A) Diagram illustrating the nuclear RNA degradation competing with export of mature transcripts. cDNA vectors differ from natural genes in that they bypass the splicing, polyadenylation, and packaging steps that form ribonucleoprotein complexes. The free mRNAs generated from cDNA vectors are more likely to be targeted for nuclear degradation and/or inefficient export. (B) Diagram showing Lac operon-controlled luciferase chimeric vectors. (C) Y-1 cells stably expressing the Lac repressor gene were transiently cotransfected with vectors shown in (B) and the control vector pRLTK. Expression of luciferase gene was induced by IPTG addition. Diagram shows luciferase activity induction time course. Data represent means ± S.D. for three transfections. The experiment was repeated twice with similar results. (D) Cytoplasmic appearance rates are calculated by doing linear regression fits on 2–24-h time points from (C).

the same molar amounts of each DNA vector (calculated by base pairs) at around 400 ng/well in 24-well plates, together with 40 ng/well of pRLTK control vector (Promega) for dual-luciferase cotransfection where applicable. This was scaled up accordingly for six-well plates. Ratio of total DNA:*Trans*It-LT1 reagent:OPTI-MEMI media is 1 μg:2·5 μl:50 μl. OPTI-MEMI media (GIBCO) were first mixed with *Trans*It-LT1 and incubated for 15 min at room temperature. DNA vectors were then added, mixed thoroughly, and incubated for another 15 min. This transfection media mixture was directly aliquoted to cells cultured in complete media with serum and incubated for 24 h. For luciferase activity measurements, cells were harvested in 1× passive lysis buffer and assayed using Promega's Dual-Luciferase kit on a Pharmingen Monolight 3010 luminometer per manufacturers' instructions.

Data from luciferase transfections are expressed as means ± S.D. calculated from the triplicate cultures.

Site-directed mutagenesis

The first, second, and the third UUAUUUAU motifs within rat StAR AURE were mutated to UUCGUUAU using the following primer pairs.

First motif 5′-CCTGCAAGGACTGCGCTTCGTTAT-GAACAGAACAACGT-3′ and 5′-ACGTT GTTCTGTTCATAACGAAGCGC AGTCCTTGCAGG-3′
Second motif 5′-CAACGTGGAACGCGTGTTTC GTTATTGAAGTCTGAAGACT-3′ and 5′-AGTCTTCAGACTTCAATAAC GAAACACGCGTTCCACGTTG-3′
Third motif 5′-TCTGAAGACTTAACAGCTGGTC GTTATTGTAATTCATTCTGACT-3′ and 5′-AGTCAGAATGAATTACAATAAC GACCAGCTGTTAAGTCTTCAGA-3′

Mutagenesis was performed using Pfu-Ultra enzyme (Stratagene) to amplify the wild-type ARE vector. PCR cycling parameters were: 30 s at 95 °C, then 18 cycles of (30 s at 95 °C, 1 min at 55 °C, 9 min at 68 °C). PCR products were extensively digested with DpnI enzyme and transformed into JM109 *Escherichia coli* competent cells. Mutant vectors were identified by sequencing.

In vitro transcription and mRNA transfection

In vitro transcription vectors for rat StARdUTR, 1·6 and 3·5 kb mRNAs were made as described previously. They were linearized with HindIII enzyme and transcribed using Ambion's mMessage mMachine T7 kit per manufacturer's protocol. The kit contains a 5′mRNA cap analog and capping enzyme activity. Transcribed messages thus is complete with a functional 5′ cap as well as 90-base poly(A) tail from the vector. Messages were checked on a denaturing agarose gel to confirm uniformly correct sizes.

mRNAs were transfected using Mirus Bio's *Trans*It-mRNA transfection kit. Cells were plated in 12-well plates at 25% density 24 h prior to transfection. One microgram mRNA was transfected in each well. The following proportion was used: 1 μg mRNA, 1 μl *Trans*It-mRNA reagent, 1 μl mRNA boost reagent, and 100 μl serum-free media. mRNA was first mixed with serum-free media, after which mRNA boost reagent was added and mixed, followed immediately by *Trans*It-mRNA reagent. The mixture was incubated at room temperature for 3 min and then aliquoted directly to cells cultured in complete media. Twelve hours after transfection when cell mRNA levels had reached a steady state, cells were washed once and changed to complete media without transfection mixture to stop uptake of transcripts and start 0-h time point. The degradation of mRNA within the cells was determined by harvesting at appropriate time points using RNeasy Mini Kit (Qiagen) and isolating total RNA according to the manufacturer's protocol. Rat StAR message levels were determined by reverse transcription and quantitative real-time PCR as described below. The half-life for each mRNA species was calculated by linear regression fit of the time points on semi-log plots. Three independent experiments were carried out for each mRNA.

IPTG induction of luciferase chimeric constructs

The LacSwitch II system from Stratagene was employed to achieve inducible expression of luciferase. Lac repressor-controlled luciferase/StAR 3′UTR vectors were made as described previously. Y-1 cells were transfected with the Lac repressor expression vector pCMVLacI by *Trans*It-LT1 as described previously. Stable clones were selected by adding 150 μg/ml hygromycin B to growth media and isolate surviving colonies after 1 month. Two stably integrated clones (Y-1 LacI cells) were obtained with this method. Lac repressor-controlled luciferase vectors were then transiently transfected into Y-1 LacI cells. IPTG was added at 5 mM concentration 24 h later to induce expression of luciferase. The experiments shown in the paper were conducted with the clone that exhibits highest induction by IPTG. Separate cultures were lysed and analyzed for luciferase activity as described previously after 2–36 h.

Western blot analysis

For StAR protein blot, cells were washed once in PBS and harvested with RIPA buffer (50 mM Tris–HCl (pH 7·4), 150 mM NaCl, 1 mM EDTA, 1 mM EGTA, 1 mM sodium vanadate, 1% NP-40, 0·25% deoxychoic acid, 0·05% SDS, 40 mM NaF, 10 mM sodium molybdate, 1 mM phenylmethanesulfonyl fluoride (PMSF), and 1% protease inhibitors cocktail from Sigma). Lysate was passed through a 25 gauge needle six times, centrifuged at 12 000 ***g*** speed for 10 min at 4 °C and supernatant collected. The lysates were assayed for protein concentrations using BCA protein assay kit (Pierce Biotechnology, Inc., Rockford, IL, USA). Sixty micrograms proteins were loaded on each lane, resolved on 10% SDS-PAGE gel, and electrophoretically transferred to nitrocellulose membranes. Following transfer, the membrane was incubated in blocking buffer tris buffered saline with tween (TBST) with 5% non-fat milk for 1 h, washed with TBST, incubated with an antibody raised against recombinant mouse StAR protein (Dr Dale Buck Hales, University of Illinois at

Chicago, USA) for 1 h, followed by three washes with TBST and incubation with horseradish peroxidase-conjugated anti-rabbit IgG containing 1% milk and another three washes. Protein bands were visualized by ECL reagent (Amersham Biosciences) and exposing the membrane against Hyperfilm (Amersham Biosciences).

Real-time RT-PCR

StAR and luciferase mRNA levels in these assays were determined by real-time RT-PCR using specific primers that bind to ORF or untranslated regions of *StAR* and luciferase genes. Total cellular RNA was isolated using RNeasy Mini Kit (Qiagen) according to the manufacturer's protocol. When mRNAs produced from transfected DNA vectors were measured, an additional step of extensive DNaseI digestion was employed to remove transfected DNA vector contamination in real-time PCR. The DNaseI treatment was performed using Qiagen's RNase-free DNase kit at 37 °C for 4 h. Effective removal of DNA vectors was confirmed by the extremely low signal of no reverse transcriptase controls in real-time PCR (<0·1% of samples with reverse transcriptase). RNA concentrations were quantitated in triplicates (<5% S.D.). Total RNA (1·5 μg) was used for cDNA synthesis by SuperscriptIII reverse transcriptase (Invitrogen) per manufacturer's protocols. cDNA products were diluted to 100 μl, from which 3 μl were used for each well in 96-well plate real-time PCR. The primer pair 5′-TGGAAGAACAAATCCCTGGGA-3′ and 5′-TGCTTTCTGTGGTAGTGCTGCA-3′ was used to amplify a 5′UTR region within rat but not mouse StAR mRNAs. To detect luciferase messages, the primer pair 5′-AGTATGGGCATTTCGCAGCC-3′ and 5′-CAACCCCTTTTTGGAAACGAAC-3′ that bind within luciferase ORF were used. Specificity of these primers was indicated by a single sharp peak within the dissociation curves. Real-time PCR was performed on a Bio-Rad MyiQ single channel real-time PCR machine, using reagents purchased from Bio-Rad. Data were collected by linked computer and analyzed using Bio-Rad MyiQ software. All samples were done in triplicates.

Results

The 3′UTR of StAR lowers protein and mRNA expression in vectors

The two transcripts produced from mouse or rat *StAR* gene share the same 5′UTR, open reading frame and a 0·7 kb region of 3′UTR. The 3·5 kb transcript contains an additional 1·9 kb extended 3′UTR (Fig. 1). To test whether the alternatively generated 3′UTRs affect StAR expression levels, we cloned cDNAs corresponding to 1·6 and 3·5 kb rat StAR mRNA into CMV promoter driven expression vectors. We also deleted the 3′UTR entirely to make a StARdUTR vector. The control vector StAR(-) (i.e. pCINeo) did not have cDNA inserts (Fig. 2A). After transfecting these vectors into steroidogenic MA-10, Y-1, and non-steroidogenic COS-1 cells, we found marked differences in the amounts of expressed StAR proteins. As shown in Fig. 2B, in MA-10 cells basal StAR is virtually undetectable. StARdUTR, StAR1.6k, and StAR3.5k express proteins in the ratio of approximately 15:5:1 as determined with the Image Quant 5.2 software. For Y-1 cells, after subtracting high basal StAR level, the pattern is similar to MA-10 cells. In COS-1 cells, StAR3.5k produces more protein than in MA-10 or Y-1 cells. There are more precursor (p37) forms in COS-1 cells, indicative of slower processing. The amounts of StAR transcripts in transfected MA-10 cells, as assessed by real-time RT-PCR, are consistent with protein levels, ruling out effects of 3′UTR on translation (Fig. 2C).

Since the transcriptional rates of these vectors are the same, the observed differences reflect effects of StAR 3′UTR on transcript cytoplasmic stability and/or the efficiency of transfer of nascent nuclear transcripts to the ribosomes. This involves competition between formation and export of ribonucleoproteins from the nucleus versus nuclear degradation of transcripts. The level of protein from StARdUTR represents 50% of that obtained by stimulation of the endogenous gene in MA-10 cells with 1 mM 8-Br-cAMP for 3 h. Strikingly, pregnenolone formation in transfected cells did not increase significantly above low basal levels (data not shown here) despite much elevated StAR protein. Recently, we also found that transfected StAR protein is rapidly and efficiently phosphorylated upon cAMP stimulation. Nevertheless, steroidogenesis rates are not enhanced (unpublished data), suggesting factors other than StAR might be rate limiting in acute steroidogenesis. Similar results were also obtained with equivalent mouse vectors. This result does not conflict with cholesterol metabolism seen with similar vectors in COS-1 cells which are low compared with even basal MA-10 activity. This deficiency is being pursued in a separate study.

StAR 5′UTR and ORF are not involved in lowering expression

We tested whether StAR 5′UTR and ORF could negatively impact mRNA levels by transfecting MA-10 cells with parallel luciferase–StAR 3′UTR chimeric constructs (Fig. 8A). Figure 8B shows that the short 3′UTR lowers luciferase expression 2·5-fold compared with the vector without 3′UTR, while the long 3′UTR reduces it almost 20-fold. In luciferase construct transfection experiments shown here and in later figures, the activity measurements directly reflect luciferase protein levels. We also measured luciferase mRNA levels produced from these vectors by real-time

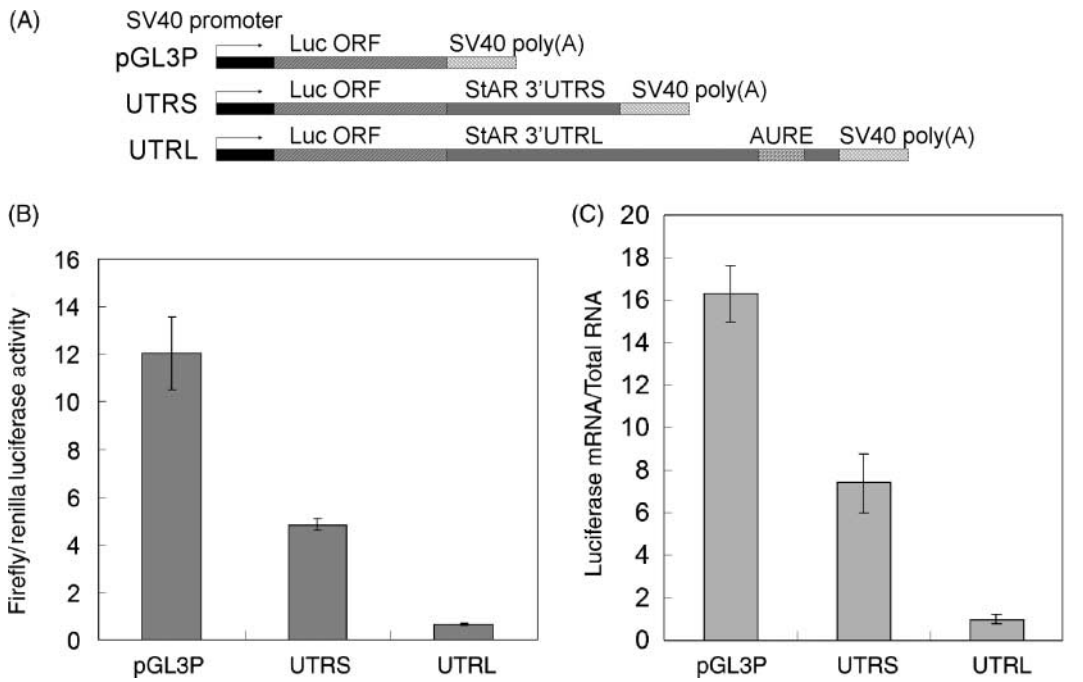

Figure 8 Effects of StAR 3′UTR on basal luciferase expression. (A) Diagram showing the parent luciferase vector and luciferase chimeric constructs. (B) Same molar amounts of vectors in (A) were cotransfected with the control vector pRLTK into MA-10 cells. Firefly and renilla luciferase activities were measured. Data represent means ± S.D. from three separate transfections. The experiment was repeated thrice with similar results. (C) Luciferase mRNA levels from transfections in (B) as quantitated by real-time RT-PCR.

RT-PCR and found them to be consistent with activity (Fig. 8C). Therefore, no translational inhibition by 3′UTR is apparent. The effects of 3′UTRs on luciferase chimeras are thus indistinguishable from those on cloned StAR vectors, including 5′UTR and ORF. We conclude that StAR 3′UTRs function the same in chimeric constructs as in native gene and that the experimental effects derive entirely from 3′UTR.

Decay kinetics of *in vitro* transcribed StAR mRNAs confirm contribution of 3′UTRs to basal instability

We sought to measure the half-lives of StAR transcripts in steroidogenic cells. Earlier reports showed that StAR messages are stabilized by transcriptional inhibitors, including actinomycin D, DRB, and α-amanitin (Clark *et al.* 1997, Zhao *et al.* 2005). This phenomenon was also observed when we used StAR or luciferase–3′UTR chimeric constructs to examine degradation of corresponding messages after transcriptional arrest (data not shown here). We therefore developed a new method to study decay kinetics of exogenous StAR transcripts. Rat StAR cDNAs with no 3′UTR, short 3′UTR (1·6 kb), or long 3′UTR (3·5 kb) were cloned into T7 promoter driven *in vitro* transcription vectors, followed by a 90-base synthetic poly(A) tail. After linearization, these vectors were transcribed *in vitro* using Ambion's T7 mMessage mMachine system. The reaction also contains 5′RNA cap analog and capping enzyme so that mRNAs generated are capped and polyadenylated as native genes. Transcription products were checked on gel and confirmed to be of uniformly correct sizes with no signs of degradation (data not shown). These rat StAR transcripts were then delivered into MA-10 cells by a liposome-based mRNA transfection method. Initial experiments showed that the transcripts reached a steady-state level within the cell after 12 h (Fig. 9A), which was determined by the balance between cellular uptake and degradation. Further mRNA uptake was then stopped by washing away the transfection media. The decline of StAR mRNA was measured by real-time RT-PCR. Transfected rat StAR was distinguished from endogenous mouse StAR transcripts using selective primers targeting a non-conserved region in 5′UTR. No signals were seen in non-transfected cells (data not shown). Figure 9B shows results from one representative experiment. The decay of transfected StAR mRNAs followed first-order kinetics. Three independent experiments were conducted and their statistics summarized in Fig. 9C. StAR3.5kb is approximately twofold more labile than StAR–no UTR, with StAR1.6kb exhibiting intermediate stability. Their half-life values are in the range of determined rates for the decline of StAR mRNA after the removal of Br-cAMP stimulus

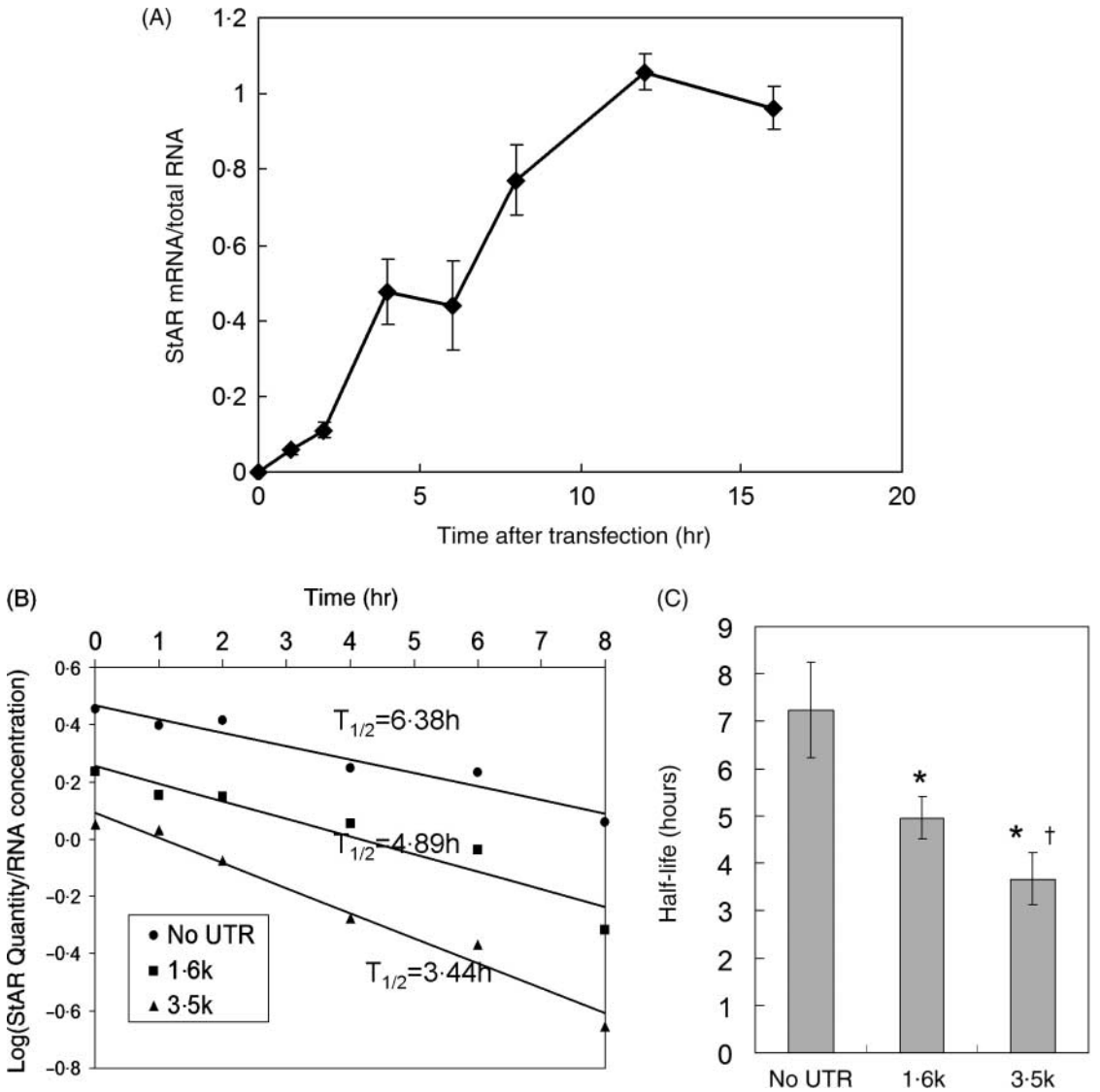

Figure 9 Half-lives of *in vitro*-transcribed StAR messages. (A) Rat StAR–no UTR mRNA was transfected into MA-10 cells. The cells were harvested at indicated time points after transfection to determine intracellular transcript levels. The 12-h time point was chosen based on the peak level. (B) Half-lives of rat StAR–no UTR, 1·6 and 3·5 kb transcripts. Representative result from one experiment is shown. Half-life for each mRNA species is determined by linear regression fitting on a semi-log plot. (C) Statistics of StAR mRNA half-lives from three independent experiments. $^{*}P<0{\cdot}05$ compared with No UTR; $^{\dagger}P<0{\cdot}05$ compared with 1·6 kb by Student's *t*-test.

(Zhao *et al.* 2005), although there the loss of 3·5 kb mRNA was about twice as rapid. Importantly, the differences between their rates of degradation are modest compared with the steady-state differences (Figs 2 and 8).

Two effects of StAR 3′UTR in expression vectors: length and sequence-specific elements

To investigate whether these differences in steady-state levels derived from the length of the 3′UTR or specific sequence features, we made antisense constructs in which the 3′UTRs were replaced with the reverse complement of the original sequences (Fig. 3A). This removes sequence-specific elements but retains effects of length and possibly some features of secondary structures determined by complementary internal sequences. These constructs were transfected into MA-10 and Y-1 cells. Figure 3B shows that in all cell types, the antisense and sense short 3′UTR vectors produced about the same level of luciferase. By contrast, the antisense long 3′UTR expressed threefold more luciferase than sense vector. The antisense long 3′UTR vector was nevertheless expressed at three times lower levels than the antisense

short 3′UTR vector. In COS-1 cells, similar trends were maintained but with smaller differences. The length of the 3′UTR alone, therefore, appears to be a factor that reduces luciferase expression levels. This will be presented in more detail in Fig. 10 where we compare the effects of several other 3′UTR modifications to dissect out the contribution of 3′UTR length to expression. The sequence-specific destabilizing effect, which manifests as differences between antisense and sense constructs, is only found with the long 3′UTR and is somewhat cell selective (Y-1 > MA-10 > COS-1). We additionally deleted the terminal 300 bases from the 2·5 kb 3′UTR which comprised the AURE region. This deletion had a modest 1·5-fold stabilizing effect on luciferase expression (Fig. 3C).

The length-dependent effect is related to appearance of cytoplasmic mRNA

These steady-state levels of mRNA are determined by the formation of cytoplasmic transcripts as well as their degradation. Although transcription from the same promoter should be the same for each vector, the formation of mature cytoplasmic transcripts additionally involves post-transcriptional nuclear processes, including splicing, polyadenylation, ribonucleoprotein packaging, and degradation which precede export to the cytoplasm for translation (Fig. 7A). In the natural gene, intron complexes that are also involved in splicing direct many of these steps, thus greatly

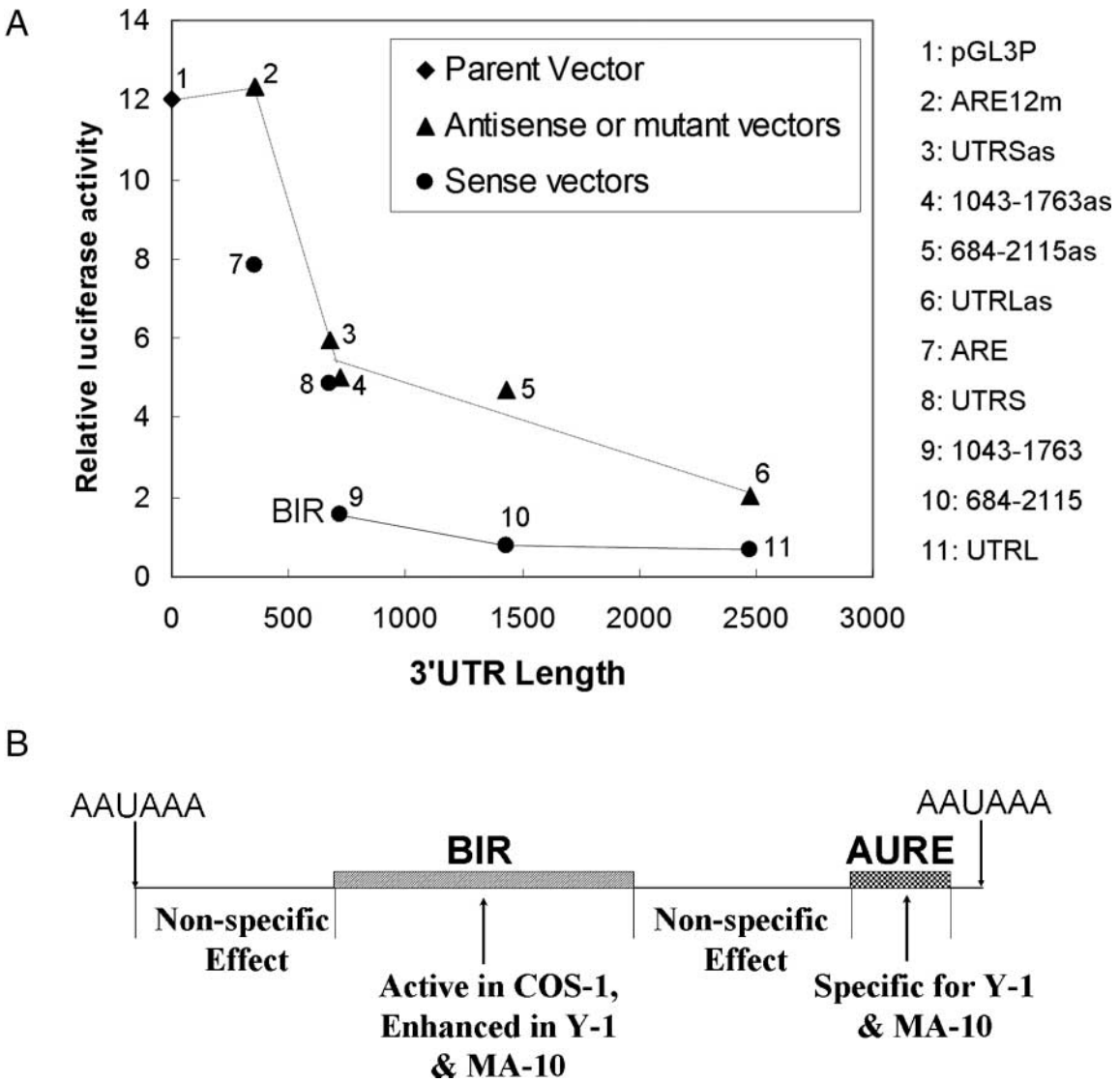

Figure 10 (A) Plot showing the relationship between chimeric constructs 3′UTR length and luciferase expression levels. The vector represented by each point is labeled. (B) Diagram summarizing instability elements within StAR extended 3′UTR and their effects in non-steroidogenic and steroidogenic cells. The lengths of the sequences are drawn approximately to scale.

enhancing the effectiveness of mRNA export relative to the transfected cDNA used here (Moore 2002, Vinciguerra & Stutz 2004). These post-transcriptional nuclear processes are likely to be substantially affected by the 3′UTR and may account for some of the steady-state expression differences described in the previous sections.

In order to assess the effect of extended 3′UTR on the rates of appearance of mRNA in the cytoplasm, we made IPTG-inducible luciferase–StAR 3′UTR chimeric vectors (Fig. 7B), in which the expression of luciferase gene is under control of the Lac operon. These constructs allow us to initiate transcription with IPTG and then assay the subsequent formation of luciferase as a measure of mRNA which reaches the cytoplasmic ribosome. We also generated Y-1 cells lines stably integrated with the Lac repressor gene (Y-1 LacI cells). After transfection into Y-1 LacI cells, these vectors show low basal luciferase expression. The addition of IPTG removes Lac repressor binding and induces each promoter. Since they are identical, IPTG should produce similar transcription rates for each vector. Based on our previous experiments, luciferase activity is directly proportional to mRNA levels (Fig. 8). The rate of increase for luciferase, therefore, measures the appearance of mRNA at the cytoplasmic ribosomes. This rate depends on the constant rate of transcription combined with the overall rate of nuclear processes that results in export to the cytoplasm. The steady-state level of mRNA is determined by this cytoplasmic appearance rate and the cytoplasmic degradation rate of the transcript. As shown in Fig. 7C, after IPTG addition, all three vectors show the same brief lag time (2 h) and then increase linearly for approximately 24 h at very different rates. The zero-order cytoplasmic appearance rates for each vector were established by fitting linear regressions to the luciferase activities from 2 to 24 h (Fig. 7D).

Table 1 summarizes the cytoplasmic appearance rates as determined from linear regression analyses of the increases seen in Fig. 7C after the constant 2-h lag period. These rates are compared with the mRNA degradation rates derived from the first-order plots shown in Fig. 9. The calculated ratio of these two rates should determine the steady-state levels generated by these constructs. As shown in Table 1, these ratios generally parallel the steady-state levels. This confirms that most of the differences in the steady-state luciferase mRNA derived from the effects of 3′UTR on post-transcription nuclear processes. By contrast, large differences in mRNA steady state caused solely by the differences in mRNA stability would be indicated by constant initial zero-order rates for transcription and post-transcriptional nuclear processes but different times to reach the steady states that are proportional to the degradation rates.

Basal destabilization conferred by AURE alone is modest but selective for steroidogenic cells

The extended StAR 3′UTR comprises two distinct sequences: an AURE of about 0·3 kb and an upstream region of about 1·4 kb. We have shown that deletion of the AURE region leads to a modest increase in luciferase expression (Fig. 3C). To further examine the effect of AURE on basal stability, we made wild-type and mutant rat AURE vectors (Fig. 5A), which have UUAUUUAU motifs mutated to disrupt interaction with destabilizing AURE-binding proteins such as TIS11b (Hudson *et al.* 2004). Figure 5B shows that in Y-1 and MA-10 cells, StAR AURE causes 40% decline in luciferase expression. This corresponds closely to the 50% increase produced by deletion of the whole AURE region (Fig. 3C). The decline is reversed by mutation of the upstream two AURE motifs. In COS-1 cells, however, the AURE sequences have no significant effect on luciferase activity. Mutation of the third UUAUUUAU motif has no further effects in any cell types. These results confirm that the AURE confers a modest effect on basal destabilization of the extended 3′UTR, but far less than 20-fold, as shown in Figs. 2 and 8. Destabilization by AURE only functions in steroidogenic cells and can be achieved with only two UUAUUUAU motifs.

Table 1 Rates of cytoplasmic mRNA appearance, degradation, and their ratios for luciferase chimeric constructs

	Relative appearance rates (h)	**First-order degradation rates** (h)	**Appearance/degradation ratio**	**Steady-state levels**
Vector				
Luc	4·84	1/6·4	9·1	16·3
Luc–UTRS	2·15	1/4·9	3·1	7·4
Luc–UTRL	1	1/3·4	1	1

Relative appearance rates are determined by linear regression fits shown in Fig. 7D. First-order degradation rates are reciprocals of mRNA half-lives from Fig. 9. The ratios are then calculated by dividing appearance rates with degradation rates and standardizing to Luc–UTRL. Steady-state levels are derived from Fig. 8C. The ratios generally correspond to steady-state levels.

A 700-base sequence upstream of the AURE region reproduces most of the destabilizing effect of the extended 3′UTR

We also examined the effect of the region upstream of AURE (684-2115) by making corresponding luciferase chimeric constructs (Fig. 4A). The results in Fig. 4B show that in steroidogenic (Y-1 and MA-10) as well as non-steroidogenic (COS-1) cells, the upstream region substantially lowered luciferase level (vector 684-2115), while the antisense vector 684-2115as exhibited threefold higher luciferase activity. This destabilization by specific sequences in the extended 3′UTR is similar to the difference between sense and antisense long 3′UTR vectors in Fig. 3B. This suggests that the region provides a sequence-specific destabilization effect that functions in parallel with the length effect shown by the antisense vectors.

To further define basal instability determinants within the upstream region, we examined separate sequences of this region (Fig. 6A, 684-1043, 684-1403, 684-1763, and 1043-1763). As shown in Fig. 6B, 684-1043 has about the same luciferase activity as the parent vector pGL3P, indicating that this region does not contribute to destabilization. The vector 1043-1763 was almost as effective as the complete upstream region, while its antisense control had threefold higher activity. The sequence between 1043 and 1763 therefore accounts for most of the sequence-specific destabilization. We designate this sequence the basal instability region (BIR).

3′UTR length-luciferase activity plot separates non-specific length effects from sequence-specific destabilizing elements

To better dissect the AURE, BIR, and length effects, we have plotted luciferase activities of several construct against their 3′UTR lengths. As shown in Fig. 10A, for sequences that do not contain the BIR, there is a general inverse relationship between steady-state expression and 3′UTR lengths when extended beyond 300–350 bases (dotted line). This appears as a minimum length of 3′UTR for the introduction of the length effect. The correlation appears to be independent of the sequences used. For example, the vectors UTRS, UTRSas, and 1043-1763as are about the same length (700 bases) and show very similar expression levels. In these constructs, only the length effect is manifested. On the other hand, 3′UTR sequences which contain the BIR (1043-1763, 684-2115, UTRL) are displaced to much lower stabilities relative to their lengths. The shape of the plots suggests that the BIR sequence is equivalent to a non-specific sequence of three to four times the length. The effect of AURE region appears as additive with the BIR/length effects. Figure 10B summarizes the BIR and the AURE sequence elements within StAR extended 3′UTR and their different effects in steroidogenic and non-steroidogenic cells.

Introns mitigate the destabilizing effects of extended StAR 3′UTR

The impact of post-transcriptional nuclear steps raises important questions about differences in these processes between transfected cDNA vectors and the natural gene. Introns are involved in many aspects of gene expression, including transcription, polyadenylation, mRNA export, localization, decay, and translational efficiency (Le Hir *et al.* 2003, Nott *et al.* 2003; see Fig. 7A). Therefore, we cloned the mouse genomic StAR locus with all six introns and complete extended 3′UTR into the same expression vector (mStAR3.5/introns, Fig. 11A). As shown in Fig. 11B and C, although it harbors the same long 3′UTR as mStAR3.5k, mStAR3.5/introns vector generates several fold more StAR protein and mRNA than mStAR3.5k, comparable with mStAR1.6k. This suggests that StAR introns enhance *StAR* gene expression. This may arise by partially offsetting the destabilizing effects of long 3′UTR or by directing polyadenylation to favor the more stable 1·6 kb transcript.

Discussion

Stimulation of rodent adrenal Y-1 and testis MA-10 cells with Br-cAMP preferentially stimulates a 3·5 kb transcript which contains an extended 3′UTR that includes three AURE motifs. AURE has been identified in over 900 human genes and is associated with the regulation of mRNA stability. In a previous paper (Zhao *et al.* 2005), we reported that the 3·5 kb transcript increases and decreases more rapidly than the 1·6 kb transcript when cAMP stimuli are applied and removed, consistent with preferential stimulation of a less stable 3·5 kb transcript. This type of regulation is typically found with genes involved in rapid cellular changes, such as early response genes (*fos*, *jun*, and *myc*), cytokines, COX2, and eNOS (Shyu *et al.* 1991, Peng *et al.* 1996, Yeilding *et al.* 1998, Rossig *et al.* 2002, Subbaramaiah *et al.* 2003). StAR as a regulator of steroidogenic responses also has a need for rapid fluctuation as hormonal stimuli change. Post-transcriptional regulation through the 3′UTR provides additional means to alter gene expression that function in parallel with transcriptional regulation through the promoter. Extensive studies have shown that the StAR promoter is regulated by multiple transcription factors (Manna *et al.* 2003). In this paper, we describe the transfection of Y-1 and MA-10 cells with a set of StAR and luciferase vectors designed

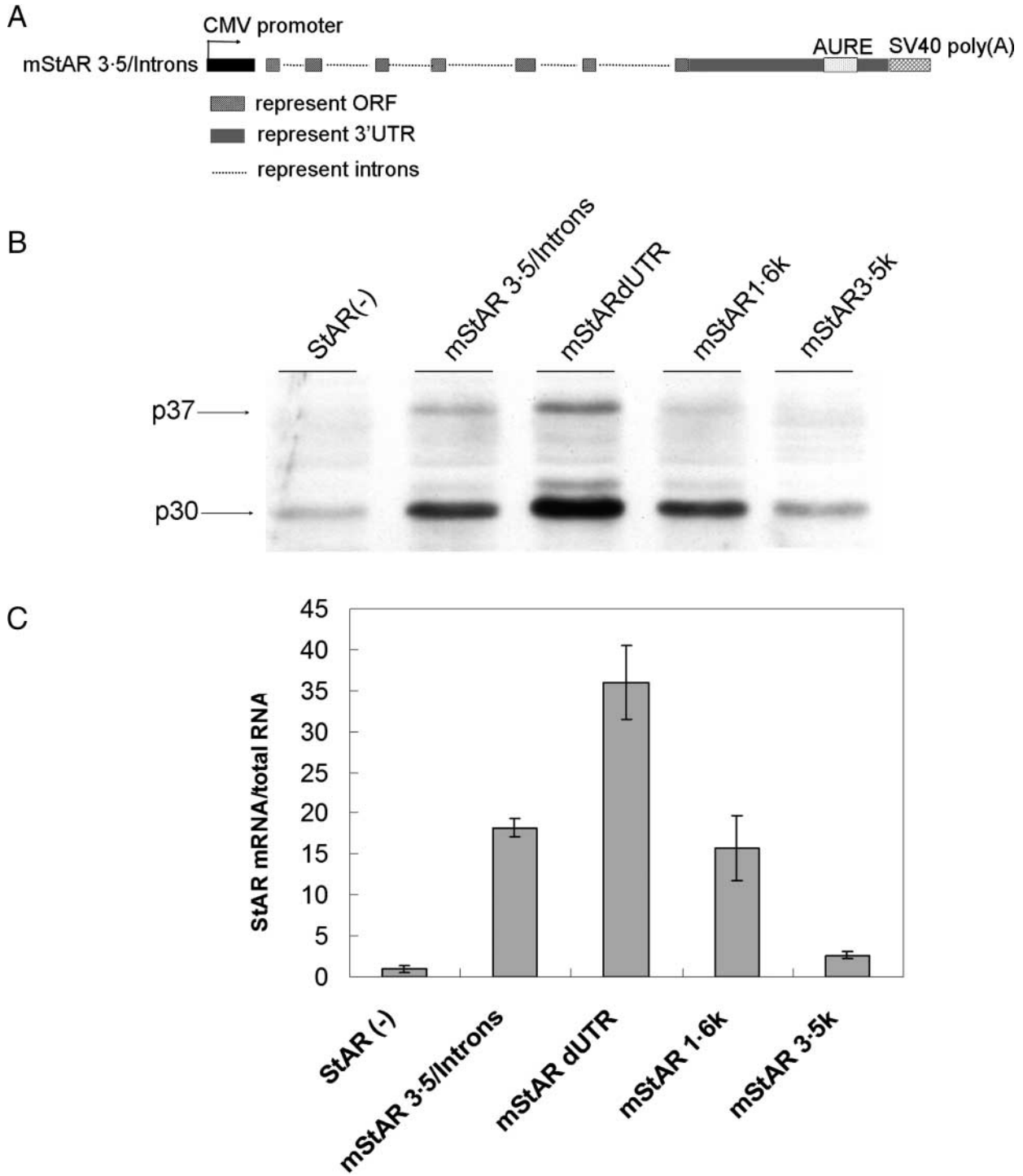

Figure 11 Intron effects on StAR expression compared with cDNA vectors. (A) Diagram showing mouse StAR construct with complete seven exons and six introns. The extended long 3′UTR is also present. (B) Vector shown in (A) was transfected into MA-10 cells along with cDNA expression vectors. StAR protein expression is analyzed by western blot. (C) StAR mRNA levels in MA-10 cells transfected with these vectors determined by real-time RT-PCR. Data represent means ± S.D. from two independent experiments.

to test the effects of 3′UTR on post-transcriptional processes. We compare vectors that share the same promoter and therefore the same rate of transcription. One model for regulation through 3′UTR is that a labile mRNA is stabilized through external stimulation of protein interactions with 3′UTR sequences. Here, we addressed *cis*-elements that affect this basal stability and whether this regulation is restricted to steroidogenic cells.

We first found that the long 3′UTR from 3·5 kb form substantially lowers StAR and luciferase protein and mRNA expression by about 20-fold. The effect of the short StAR 3′ UTR was only two- to threefold (Figs 2 and 8). Since the differences are similar for either StAR or luciferase, they are due solely to effects of the extended 3′UTR. The differences are similar for mRNA and protein and therefore do not reflect the effects of 3′UTR on translation. The effects of 3′UTR on expression were also retained in the non-steroidogenic COS-1 cells although with smaller differences. Thus, the downregulation of transcripts containing the extended StAR 3′UTR is preferentially enhanced by factors in steroidogenic cell lines but is not specific to these cells.

The long 3′UTR constructs retain the internal poly(A) signal used to generate the short form. However, we have previously shown that changes in the 3·5 kb mRNA derived from the StAR3.5 vector were similar whether we used primer pairs targeted to the extended 3′UTR or to the ORF (Zhao *et al.* 2005). Thus, intermediate polyadenylation appears to be minimal from cDNA vectors, in contrast to the natural gene. The strong SV40 poly(A) signal, which is inserted in all these constructs may also favor terminal polyadenylation (Carswell & Alwine 1989, Legendre & Gautheret 2003). The SV40 poly(A) signal enhances the expression of these StAR vectors compared with those containing only the natural polyadenylation signals (Zhao *et al.* 2005). Data presented here and in the previous paper suggest that SV40 polyadenylation may be more effective for short 3′UTR.

StAR mRNA turnover in Y-1 cells is completely halted by transcriptional inhibitors (Zhao *et al.* 2005). We confirmed this finding by showing that the addition of actinomycin D to StAR expression vectors resulted in extremely slow mRNA degradation (half times >10 h, data not shown). This apparent dependence of mRNA stability on transcription has been reported previously for other labile mRNA but has not been well explained (Goldberg *et al.* 1991, Stacey *et al.* 1994, Foster *et al.* 2001). Since this typical approach was excluded, we used direct transfection of *in vitro*-transcribed StAR mRNA into MA-10 cells to measure mRNA degradation rates. The first-order rates indicated that StAR mRNAs are destabilized by the extended 3′UTR (Fig. 9), but the modest effects were too small (twofold) to account for the steady-state differences (20-fold) seen with expression vectors. The degradation half-times (3·5 h for 3·5 kb and 5 h for 1·6 kb) were, however, similar to those seen in Y-1 cells after the removal of the Br-cAMP stimulus (2 and 4 h; Zhao *et al.* 2005).

The large effects of 3′UTR on steady-state mRNA levels occur after the shared transcription process and prior to translation. IPTG initiation of Lac-suppressed luciferase/StAR chimeras showed a 2-h delay independent of 3′UTR which precedes the induction (Fig. 7). This presumably reflects the time for LacO derepression and promoter activation, which should be similar for each of these constructs. We have established that the increase in expression of luciferase then follows zero-order rates that were greatly attenuated by the long 3′UTR. This fivefold slower cytoplasmic appearance rate coupled with the twofold faster degradation accounts for a tenfold lower steady-state level, which closely matches the 15 to 20-fold observed differences (Table 1). The maintenance of widely different zero-order rates for similar durations is also completely inconsistent with a dominant influence of cytoplasmic mRNA degradation. Instead, the reduced rates reflect decreased efficiency in nuclear processes between transcription and entry into the cytoplasm. Polyadenylation and formation of RNA-protein complexes prior to nuclear export compete with nuclear degradation (Vinciguerra & Stutz 2004). Polyadenylation clearly plays a role since we previously showed that the inclusion of the SV40 polyadenylation signal appreciably elevated the steady states (Zhao *et al.* 2005). Our data provide evidence that the long 3′UTR decreases the delivery of mRNA to the cytoplasm by favoring the nuclear degradation process.

We have systematically manipulated the 3′UTR of luciferase chimeras to resolve several 3′UTR sequence contributions that each selectively diminish expression of 3·5 kb StAR mRNA. A set of antisense 3′UTR constructs indicated that increased 3′UTR length produces a non-specific decrease in stability (Fig. 10), which accounts for all the effect of the short 3′UTR and some of the loss produced by the long 3′UTR. This length effect is seen in COS-1 cells although less than in Y-1 and MA-10 cells. The diminished expression difference between short and long StAR 3′UTR with endogenous polyadenylation may arise from stimulation of this length effect by the inserted SV40 signal. Sequence-specific destabilization further contributes to threefold destabilization by long 3′UTR (Fig. 3).

We have resolved two sequence-specific mechanisms. Deletion of the AURE or separate introduction into a luciferase chimera indicated that the isolated AURE caused a modest decrease in basal stability (40%) that was selective for steroidogenic cells (Fig. 5). The destabilization effect was removed by mutation of two of the AURE motifs. The adjacent upstream region

surprisingly produced much greater losses in expression. A sequence of 700 bases (1043-1763) produced an appreciably large destabilizing effect on the extended 3′UTR (Fig. 6). We termed this the basal instability region (BIR). In Fig. 10, we show that destabilization by the extended 3′UTR that contains BIR exhibits a parallel length effect but with an enhanced effectiveness of about fourfold. We were concerned that the use of antisense sequences could retain RNA secondary structures. However, several different sequences of about 700 bases produce similar effects. This confirms that the length effects are relatively non-specific. Increased spacing between stop condon and poly(A) tail can diminish the formation of export-competent ribonucleoprotein complexes. This could favor nuclear exosome degradation (Colgan & Manley 1997) and account for the non-specific length effect.

The minimally functional sequences of BIR are still unknown. We used the *m*fold web server to examine possible RNA secondary structures of BIR (Zuker 2003). Some internal basepairings and non-paired loops were predicted, but no particular strong secondary structures were identified. Furthermore, antisense BIR sequences, which should retain most of the secondary structural features of BIR, show threefold higher luciferase expression level (Fig. 6B). This argues against a role of secondary structure in the destabilizing effect of BIR. We also aligned the rat BIR sequences with the corresponding mouse StAR 3′UTR, and found a region of about 300 bases that is over 80% identical, with three other shorter regions (25–100 bases) also showing >80% identity. Whether these sequences harbor *cis*-elements that mediate BIR's destabilizing effect awaits future examination. One possible hypothesis for the mechanism of BIR is that this region may contain targets for endogenous miRNA. Indeed, our search of BIR against the Sanger Institute's miRNA database returned one mature miRNA (mmu-miR-706) with only one base mismatch, although the miRNA is from a murine database. It is possible that more complete miRNA databases in the future will help identify potential targets within BiR.

We hypothesize that destabilization by BIR is enhanced in steroidogenic cells, rendering the 3·5 kb transcript more labile under basal conditions and primed for fast stabilization responses to external stimuli. The AURE contributes only modestly to these basal stability mechanisms. Recent studies using bovine adrenocortical cells indicate that AURE in VEGF responds to stabilization by cAMP activation of HuR and destabilization by TIS11b. These proteins compete for AURE sequences (Cherradi *et al.* 2006). The AURE in the StAR 3′UTR match the consensus binding site for TIS11b homodimers (Ciais *et al.* 2004). Another AURE-binding protein AUF1 has also been implicated in regulation of mRNA stability (Raineri *et al.* 2004). We have recently found that each of these proteins is highly expressed in MA-10 and Y-1 cells (unpublished data).

In higher eukaryotes, introns have been reported to affect many stages of gene expression, including transcription, polyadenylation, mRNA export, translation, and mRNA turnover (Le Hir *et al.* 2001, Furger *et al.* 2002, Proudfoot *et al.* 2002, Wilkinson & Shyu 2002). The magnitude of intron effects varies among genes and is dependent on their locations (Nott *et al.* 2003). The low expression derived from the 3·5 kb cDNA vector prompted us to ask whether the endogenous *StAR* gene had mechanisms to enhance transcript formation. Our results with a cloned minigene clearly show that introns enhance StAR expression, partially counteracting the destabilization of the extended 3′UTR (Fig. 11). However, since we have not identified the transcripts we cannot exclude the possibility that introns affect polyadenylation to produce the more stabile 1·6 kb transcript.

Artificially long mRNA half-lives measured by transcriptional inhibitors have previously been reported. This may be a more wide spread problem than often noticed (Goldberg *et al.* 1991, Stacey *et al.* 1994, Foster *et al.* 2001). We have developed methods which accurately reflect the rapid responses seen in steroidogenic cells and have shown that the 3·5 kb message is indeed less stable basally than the 1·6 kb message (Fig. 9). Alternative polyadenylation is a common yet poorly studied phenomenon (Edwalds-Gilbert *et al.* 1997, Beaudoing *et al.* 2000). In some instances, it has been established that messages generated by this mechanism harbor distinct 3′UTR sequence elements with important regulatory implications (Touriol *et al.* 1999, Caballero *et al.* 2004, Hall-Pogar *et al.* 2005). Our results suggest the same applies to rodent *StAR* gene. Based on all the information, we hypothesize that the 3·5 kb message serves as a fast responder to external stimuli due to its intrinsically short half-life conferred by BIR and potential regulation through AURE, while the 1·6 kb message reacts more slowly to establish a baseline expression level. The combination of these two responses makes the *StAR* gene adaptable to a variety of physiological conditions and steroidogenic needs.

Acknowledgements

We thank Dr Dale Buck Hales at the University of Illinois at Chicago for providing us with the StAR antibody, and Dr James Malter at the University of Wisconsin-Madison for the pBSKpA.1B *in vitro* transcription vector as well as his suggestions on mRNA stability studies. The authors declare that there is no conflict of interest that would prejudice the impartiality of this scientific work.

References

Arakane F, Sugawara T, Nishino H, Liu Z, Holt JA, Pain D, Stocco DM, Miller WL & Strauss JF III 1996 Steroidogenic acute regulatory protein (StAR) retains activity in the absence of its mitochondrial import sequence: implications for the mechanism of StAR action. *PNAS* **93** 13731–13736.

Ariyoshi N, Kim Y-C, Artemenko I, Bhattacharyya KK & Jefcoate CR 1998 Characterization of the rat StAR gene that encodes the predominant 3.5-kilobase pair mRNA. ACTH stimulation of adrenal steroids *in vivo* precedes elevation of StAR mRNA and protein. *Journal of Biological Chemistry* **273** 7610–7619.

Artemenko IP, Zhao D, Hales DB, Hales KH & Jefcoate CR 2001 Mitochondrial processing of newly synthesized steroidogenic acute regulatory protein (StAR), but not total StAR, mediates cholesterol transfer to cytochrome P450 side chain cleavage enzyme in adrenal cells. *Journal of Biological Chemistry* **276** 46583–46596.

Beaudoing E, Freier S, Wyatt JR, Claverie JM & Gautheret D 2000 Patterns of variant polyadenylation signal usage in human genes. *Genome Research* **10** 1001–1010.

Bevilacqua A, Ceriani MC, Capaccioli S & Nicolin A 2003 Post-transcriptional regulation of gene expression by degradation of messenger RNAs. *Journal of Cellular Physiology* **195** 356–372.

Bose H, Lingappa VR & Miller WL 2002 Rapid regulation of steroidogenesis by mitochondrial protein import. *Nature* **417** 87–91.

Brennan CM & Steitz JA 2001 HuR and mRNA stability. *Cellular and Molecular Life Sciences* **58** 266–277.

Buhman KF, Accad M & Farese RV 2000 Mammalian acyl-CoA:cholesterol acyltransferases. *Biochimica et Biophysica Acta* **1529** 142–154.

Caballero JJ, Giron MD, Vargas AM, Sevillano N, Suarez MD & Salto R 2004 AU-rich elements in the mRNA 3′-untranslated region of the rat receptor for advanced glycation end products and their relevance to mRNA stability. *Biochemical and Biophysical Research Communications* **319** 247–255.

Caron KM, Soo SC, Wetsel WC, Stocco DM, Clark BJ & Parker KL 1997 Targeted disruption of the mouse gene encoding steroidogenic acute regulatory protein provides insights into congenital lipoid adrenal hyperplasia. *PNAS* **94** 11540–11545.

Carswell S & Alwine JC 1989 Efficiency of utilization of the simian virus 40 late polyadenylation site: effects of upstream sequences. *Molecular and Cellular Biology* **9** 4248–4258.

Cherradi N, Lejczak C, Desroches-Castan A & Feige JJ 2006 Antagonistic functions of tetradecanoyl phorbol acetate-inducible-sequence 11b and HuR in the hormonal regulation of vascular endothelial growth factor messenger ribonucleic acid stability by adrenocorticotropin. *Molecular Endocrinology* **20** 916–930.

Ciais D, Cherradi N, Bailly S, Grenier E, Berra E, Pouyssegur J, Lamarre J & Feige JJ 2004 Destabilization of vascular endothelial growth factor mRNA by the zinc-finger protein TIS11b. *Oncogene* **23** 8673–8680.

Clark BJ, Wells J, King SR & Stocco DM 1994 The purification, cloning, and expression of a novel luteinizing hormone-induced mitochondrial protein in MA-10 mouse Leydig tumor cells. Characterization of the steroidogenic acute regulatory protein (StAR). *Journal of Biological Chemistry* **269** 28314–28322.

Clark BJ, Soo SC, Caron KM, Ikeda Y, Parker KL & Stocco DM 1995 Hormonal and developmental regulation of the steroidogenic acute regulatory protein. *Molecular Endocrinology* **9** 1346–1355.

Clark BJ, Combs R, Hales KH, Hales DB & Stocco DM 1997 Inhibition of transcription affects synthesis of steroidogenic acute regulatory protein and steroidogenesis in MA-10 mouse Leydig tumor cells. *Endocrinology* **138** 4893–4901.

Clem BF & Clark BJ 2006 Association of the mSin3A-histone deacetylase 1/2 corepressor complex with the mouse steroidogenic acute regulatory protein gene. *Molecular Endocrinology* **20** 100–113.

Colgan DF & Manley JL 1997 Mechanism and regulation of mRNA polyadenylation. *Genes and Development* **11** 2755–2766.

Cornejo Maciel F, Maloberti P, Neuman I, Cano F, Castilla R, Castillo F, Paz C & Podesta EJ 2005 An arachidonic acid-preferring acyl-CoA synthetase is a hormone-dependent and obligatory protein in the signal transduction pathway of steroidogenic hormones. *Journal of Molecular Endocrinology* **34** 655–666.

DiBartolomeis MJ & Jefcoate CR 1984 Characterization of the acute stimulation of steroidogenesis in primary bovine adrenal cortical cell cultures. *Journal of Molecular Endocrinology* **259** 10159–10167.

Edwalds-Gilbert G, Veraldi KL & Milcarek C 1997 Alternative poly(A) site selection in complex transcription units: means to an end? *Nucleic Acids Research* **25** 2547–2561.

Epstein LF & Orme-Johnson NR 1991 Regulation of steroid hormone biosynthesis. Identification of precursors of a phosphoprotein targeted to the mitochondrion in stimulated rat adrenal cortex cells. *Journal of Biological Chemistry* **266** 19739–19745.

Ferguson JJ Jr 1963 Protein synthesis and adrenocorticotropin responsiveness. *Journal of Biological Chemistry* **238** 2754–2759.

Foster D, Strong R & Morgan WW 2001 A tetracycline-repressible transactivator approach suggests a shorter half-life for tyrosine hydroxylase mRNA. *Brain Research. Brain Research Protocols* **7** 137–146.

Fujieda K, Okuhara K, Abe S, Tajima T, Mukai T & Nakae J 2003 Molecular pathogenesis of lipoid adrenal hyperplasia and adrenal hypoplasia congenita. *Journal of Steroid Biochemistry and Molecular Biology* **85** 483–489.

Furger A, O'Sullivan JM, Binnie A, Lee BA & Proudfoot NJ 2002 Promoter proximal splice sites enhance transcription. *Genes and Development* **16** 2792–2799.

Goldberg MA, Gaut CC & Bunn HF 1991 Erythropoietin mRNA levels are governed by both the rate of gene transcription and posttranscriptional events. *Blood* **77** 271–277.

Guhaniyogi J & Brewer G 2001 Regulation of mRNA stability in mammalian cells. *Gene* **265** 11–23.

Hall-Pogar T, Zhang H, Tian B & Lutz CS 2005 Alternative polyadenylation of cyclooxygenase-2. *Nucleic Acids Research* **33** 2565–2579.

Hauet T, Yao ZX, Bose HS, Wall CT, Han Z, Li W, Hales DB, Miller WL, Culty M & Papadopoulos V 2005 Peripheral-type benzodiazepine receptor-mediated action of steroidogenic acute regulatory protein on cholesterol entry into leydig cell mitochondria. *Molecular Endocrinology* **19** 540–554.

Hirakawa T, Galet C & Ascoli M 2002 MA-10 cells transfected with the human lutropin/choriogonadotropin receptor (hLHR): a novel experimental paradigm to study the functional properties of the hLHR. *Endocrinology* **143** 1026–1035.

Hiroi H, Christenson LK, Chang L, Sammel MD, Berger SL & Strauss JF III 2004 Temporal and spatial changes in transcription factor binding and histone modifications at the steroidogenic acute regulatory protein (StAR) locus associated with StAR transcription. *Molecular Endocrinology* **18** 791–806.

Hudson BP, Martinez-Yamout MA, Dyson HJ & Wright PE 2004 Recognition of the mRNA AU-rich element by the zinc finger domain of TIS11d. *Nature Structural and Molecular Biology* **11** 257–264.

King SR, Liu Z, Soh J, Eimerl S, Orly J & Stocco DM 1999 Effects of disruption of the mitochondrial electrochemical gradient on steroidogenesis and the steroidogenic acute regulatory (StAR) protein. *Journal of Steroid Biochemistry and Molecular Biology* **69** 143–154.

Kraemer FB, Shen WJ, Harada K, Patel S, Osuga J, Ishibashi S & Azhar S 2004 Hormone-sensitive lipase is required for high-density lipoprotein cholesteryl ester-supported adrenal steroidogenesis. *Molecular Endocrinology* **18** 549–557.

Krueger RJ & Orme-Johnson NR 1983 Acute adrenocorticotropic hormone stimulation of adrenal corticosteroidogenesis. Discovery of a rapidly induced protein. *Journal of Biological Chemistry* **258** 10159–10167.

Le Hir H, Gatfield D, Izaurralde E & Moore MJ 2001 The exon–exon junction complex provides a binding platform for factors involved in mRNA export and nonsense-mediated mRNA decay. *EMBO Journal* **20** 4987–4997.

Le Hir H, Nott A & Moore MJ 2003 How introns influence and enhance eukaryotic gene expression. *Trends in Biochemical Sciences* **28** 215–220.

Legendre M & Gautheret D 2003 Sequence determinants in human polyadenylation site selection. *BMC Genomics* **4** 7.

Liu J, Li H & Papadopoulos V 2003 PAP7, a PBR/PKA-RIalpha-associated protein: a new element in the relay of the hormonal induction of steroidogenesis. *Journal of Steroid Biochemistry and Molecular Biology* **85** 275–283.

Manna PR, Wang XJ & Stocco DM 2003 Involvement of multiple transcription factors in the regulation of steroidogenic acute regulatory protein gene expression. *Steroids* **68** 1125–1134.

Moore MJ 2002 Nuclear RNA turnover. *Cell* **108** 431–434.

Nott A, Meislin SH & Moore MJ 2003 A quantitative analysis of intron effects on mammalian gene expression. *RNA* **9** 607–617.

Peng S, Chen C & Shyu A 1996 Functional characterization of a non-AUUUA AU-rich element from the c-jun proto-oncogene mRNA: evidence for a novel class of AU-rich elements. *Molecular and Cellular Biology* **16** 1490–1499.

Pon LA, Hartigan JA & Orme-Johnson NR 1986 Acute ACTH regulation of adrenal corticosteroid biosynthesis. Rapid accumulation of a phosphoprotein. *Journal of Biological Chemistry* **261** 13309–13316.

Privalle CT, Crivello JF & Jefcoate CR 1983 Regulation of intramitochondrial cholesterol transfer to side-chain cleavage cytochrome P-450 in rat adrenal gland. *PNAS* **80** 702–706.

Proudfoot NJ, Furger A & Dye MJ 2002 Integrating mRNA processing with transcription. *Cell* **108** 501–512.

Raineri I, Wegmueller D, Gross B, Certa U & Moroni C 2004 Roles of AUF1 isoforms HuR and BRF1 in ARE-dependent mRNA turnover studied by RNA interference. *Nucleic Acids Research* **32** 1279–1288.

Rossig L, Li H, Fisslthaler B, Urbich C, Fleming I, Forstermann U, Zeiher AM & Dimmeler S 2002 Inhibitors of histone deacetylation downregulate the expression of endothelial nitric oxide synthase and compromise endothelial cell function in vasorelaxation and angiogenesis. *Circulation Research* **91** 837–844.

Rusovici R, Hui YY & Lavoie HA 2005 Epidermal growth factor-mediated inhibition of follicle-stimulating hormone-stimulated *StAR* gene expression in porcine granulosa cells is associated with reduced histone H3 acetylation. *Biology of Reproduction* **72** 862–871.

Shyu A, Belasco J & Greenberg M 1991 Two distinct destabilizing elements in the c-fos message trigger deadenylation as a first step in rapid mRNA decay. *Genes and Development* **5** 221–231.

Stacey KJ, Nagamine Y & Hume DA 1994 RNA synthesis inhibition stabilises urokinase mRNA in macrophages. *FEBS Letters* **356** 311–313.

Stocco DM & Sodeman TC 1991 The 30-kDa mitochondrial proteins induced by hormone stimulation in MA-10 mouse Leydig tumor cells are processed from larger precursors. *Journal of Biological Chemistry* **266** 19731–19738.

Subbaramaiah K, Marmo TP, Dixon DA & Dannenberg AJ 2003 Regulation of cyclooxgenase-2 mRNA stability by taxanes: evidence for involvement of p38, MAPKAPK-2, and HuR. *Journal of Biological Chemistry* **278** 37637–37647.

Sugawara T, Holt JA, Driscoll D, Strauss JF III, Lin D, Miller WL, Patterson D, Clancy KP, Hart IM, Clark BJ *et al.* 1995 Human steroidogenic acute regulatory protein: functional activity in COS-1 cells, tissue-specific expression, and mapping of the structural gene to 8p11.2 and a pseudogene to chromosome 13. *PNAS* **92** 4778–4782.

Sugawara T, Shimizu H, Hoshi N, Nakajima A & Fujimoto S 2003 Steroidogenic acute regulatory protein-binding protein cloned by a yeast two-hybrid system. *Journal of Biological Chemistry* **278** 42487–42494.

Sun HS, Hsiao KY, Hsu CC, Wu MH & Tsai SJ 2003 Transactivation of steroidogenic acute regulatory protein in human endometriotic stromal cells is mediated by the prostaglandin EP2 receptor. *Endocrinology* **144** 3934–3942.

Temel RE, Trigatti B, DeMattos RB, Azhar S, Krieger M & Williams DL 1997 Scavenger receptor class B, type I (SR-BI) is the major route for the delivery of high density lipoprotein cholesterol to the steroidogenic pathway in cultured mouse adrenocortical cells. *PNAS* **94** 13600–13605.

Touriol C, Morillon A, Gensac MC, Prats H & Prats AC 1999 Expression of human fibroblast growth factor 2 mRNA is post-transcriptionally controlled by a unique destabilizing element present in the 3'-untranslated region between alternative polyadenylation sites. *Journal of Biological Chemistry* **274** 21402–21408.

Tsujishita Y & Hurley JH 2000 Structure and lipid transport mechanism of a StAR-related domain. *Nature Structural Biology* **7** 408–414.

Vinciguerra P & Stutz F 2004 mRNA export: an assembly line from genes to nuclear pores. *Current Opinion in Cell Biology* **16** 285–292.

Wilkinson MF & Shyu AB 2002 RNA surveillance by nuclear scanning? *Nature Cell Biology* **4** E144–E147.

Wilusz CJ & Wilusz J 2004 Bringing the role of mRNA decay in the control of gene expression into focus. *Trends in Genetics* **20** 491–497.

Yeilding NM, Procopio WN, Rehman MT & Lee WM 1998 c-myc mRNA is down-regulated during myogenic differentiation by accelerated decay that depends on translation of regulatory coding elements. *Journal of Biological Chemistry* **273** 15749–15757.

Zhao D, Duan H, Kim YC & Jefcoate CR 2005 Rodent StAR mRNA is substantially regulated by control of mRNA stability through sites in the 3'-untranslated region and through coupling to ongoing transcription. *Journal of Steroid Biochemistry and Molecular Biology* **96** 155–173.

Zuker M 2003 *M*fold web server for nucleic acid folding and hybridization prediction. *Nucleic Acids Research* **31** 3406–3415.

Received 13 September 2006
Accepted 9 October 2006
Made available online as an Accepted Preprint 14 November 2006